Module 5 : Lecture 1
VISCOUS INCOMPRESSIBLE FLOW
(Fundamental Aspects)

Overview

Being highly non-linear due to the convective acceleration terms, the *Navier-Stokes* equations are difficult to handle in a physical situation. Moreover, there are no general analytical schemes for solving the nonlinear partial differential equations. However, there are few applications where the convective acceleration vanishes due to the nature of the geometry of the flow system. So, the exact solutions are often possible. Since, the *Navier-Stokes* equations are applicable to *laminar and turbulent flow*s, the complication again arise due to fluctuations in velocity components for turbulent flow. So, these exact solutions are referred to laminar flows for which the velocity is independent of time (steady flow) or dependent on time (unsteady flow) in a well-defined manner. The solutions to these categories of the flow field can be applied to the *internal and external flows*. The flows that are bounded by walls are called as internal flows while the external flows are unconfined and free to expand. The classical example of internal flow is the pipe/duct flow while the flow over a flat plate is considered as external flow. Few classical cases of flow fields will be discussed in this module pertaining to internal and external flows.

Laminar and Turbulent Flows

The fluid flow in a duct may have three characteristics denoted as laminar, turbulent and transitional. The curves shown in Fig. 5.1.1, represents the *x*-component of the velocity as a function of time at a point 'A' in the flow. For laminar flow, there is one component of velocity $\vec{V} = u\,\hat{i}$ and random component of velocity normal to the axis becomes predominant for turbulent flows i.e. $\vec{V} = u\,\hat{i} + v\,\hat{j} + w\hat{k}$. When the flow is laminar, there are occasional disturbances that damps out quickly. The flow Reynolds number plays a vital role in deciding this characteristic. Initially, the flow may start with laminar at moderate Reynolds number. With subsequent increase in Reynolds number, the orderly flow pattern is lost and fluctuations become more predominant. When the Reynolds number crosses some limiting value, the flow is characterized as turbulent. The changeover phase is called as *transition to turbulence*. Further, if the

Reynolds number is decreased from turbulent region, then flow may come back to the laminar state. This phenomenon is known as *relaminarization*.

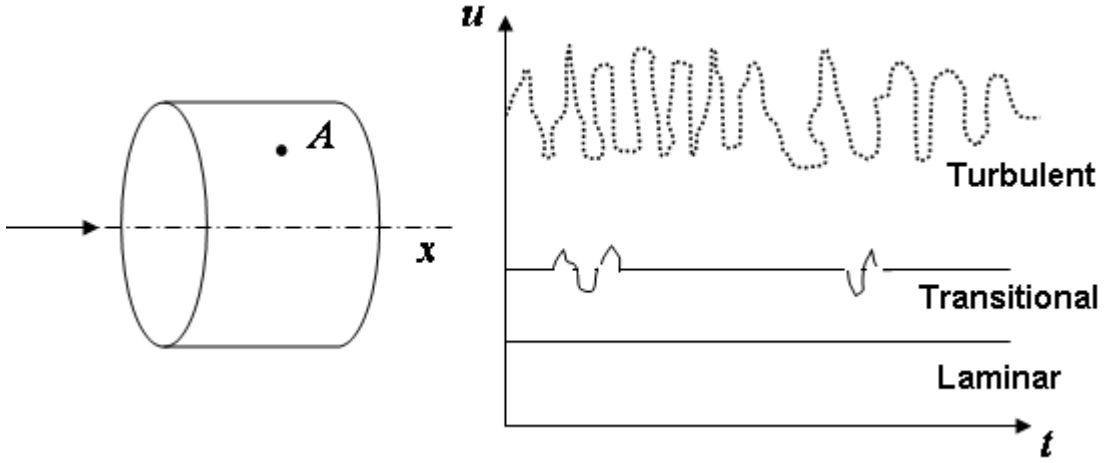

Fig. 5.1.1: Time dependent fluid velocity at a point.

The primary parameter affecting the transition is the Reynolds number defined as, $\mathrm{Re} = \frac{\rho UL}{\mu}$ where, U is the average stream velocity and L is the characteristics length/width. The flow regimes may be characterized for the following approximate ranges;

$0 < \mathrm{Re} < 1$: Highly viscous laminar motion

$1 < \mathrm{Re} < 100$: Laminar and Reynolds number dependence

$10^2 < \mathrm{Re} < 10^3$: Laminar boundary layer

$10^3 < \mathrm{Re} < 10^4$: Transition to turbulence

$10^4 < \mathrm{Re} < 10^6$: Turbulent boundary layer

$\mathrm{Re} > 10^6$: Turbulent and Reynolds number dependence

Fully Developed Flow

The fully developed steady flow in a pipe may be driven by gravity and /or pressure forces. If the pipe is held horizontal, gravity has no effect except for variation in hydrostatic pressure. The pressure difference between the two sections of the pipe, essentially drives the flow while the viscous effects provides the restraining force that exactly balances the pressure forces. This leads to the fluid moving with constant velocity (no acceleration) through the pipe. If the viscous forces are absent, then pressure will remain constant throughout except for hydrostatic variation.

In an internal flow through a long duct is shown in Fig. 5.1.2. There is an entrance *region* where the inviscid upstream flow converges and enters the tube. The viscous boundary layer grows downstream, retards the axial flow $\left[u(r,x)\right]$ at the wall and accelerates the core flow in the center by maintaining the same flow rate.

$$Q = \int u\, dA = \text{constant} \tag{5.1.1}$$

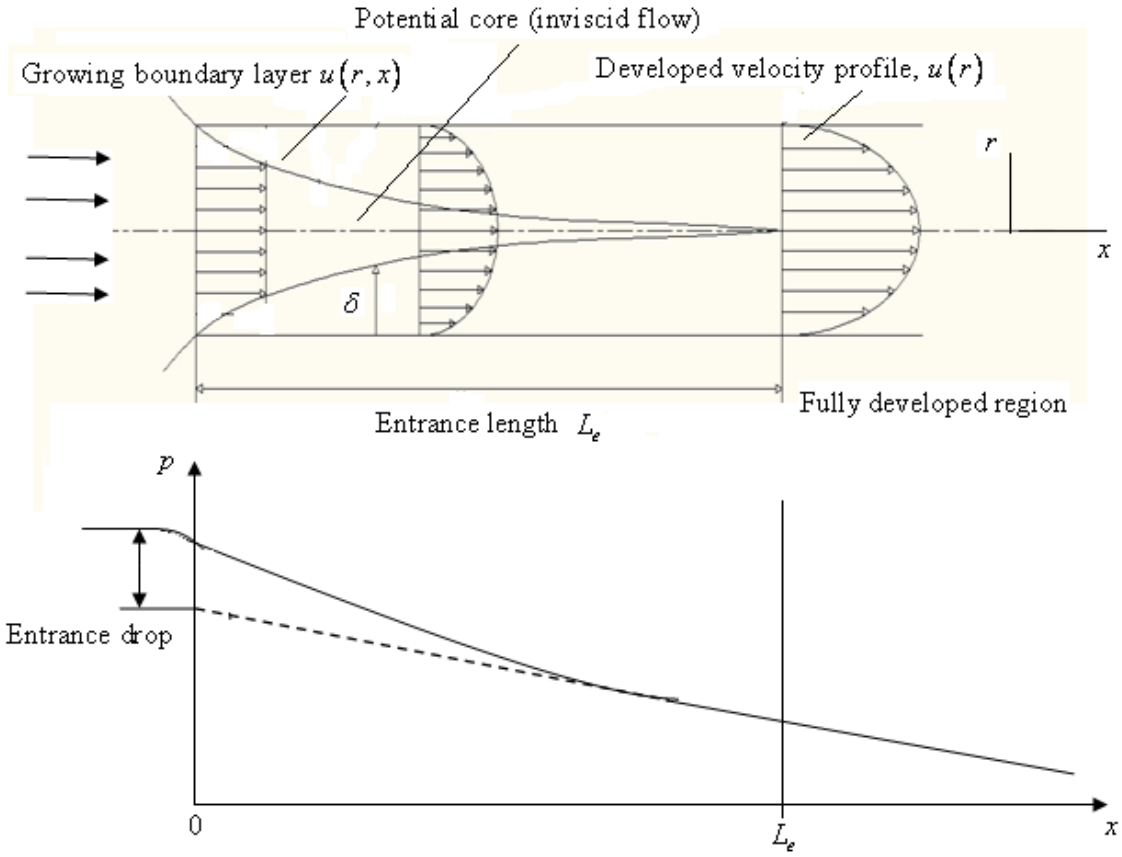

Fig. 5.1.2: Velocity profile and pressure changes in a duct flow.

At a finite distance from entrance, the boundary layers form top and bottom wall merge as shown in Fig. 5.1.2 and the inviscid core disappears, thereby making the flow entirely viscous. The axial velocity adjusts slightly till the entrance length is reached $\left(x = L_e\right)$ and the velocity profile no longer changes in x and $u \approx u\left(r\right)$ only. At this stage, the flow is said to be fully-developed for which the velocity profile and wall shear remains constant. Irrespective of laminar or turbulent flow, the pressure drops linearly with x. The typical velocity and temperature profile for laminar fully developed flow in a pipe is shown in Fig. 5.1.2. The most accepted correlations for entrance length in a flow through pipe of diameter $\left(d\right)$, are given below;

$$
\begin{aligned}
&L_e = f\left(d, V, \rho, \mu\right); \quad V = Q/A \\
&\text{so that } L_e = \left(\frac{\rho V d}{\mu}\right) = g\left(\mathrm{Re}\right) \\
&\text{Laminar flow}: \ \frac{L_e}{d} \approx 0.06 \ \mathrm{Re} \\
&\text{Turbulent flow}: \frac{L_e}{d} \approx 4.4 \left(\mathrm{Re}\right)^{\frac{1}{6}}
\end{aligned}
\tag{5.1.2}
$$

Laminar and Turbulent Shear

In the absence of thermal interaction, one needs to solve continuity and momentum equation to obtain pressure and velocity fields. If the density and viscosity of the fluids is assumed to be constant, then the equations take the following form;

$$
\begin{aligned}
&\text{Continuity: } \frac{\partial u}{\partial x} + \frac{\partial v}{\partial y} + \frac{\partial w}{\partial z} = 0 \\
&\text{Momentum: } \rho \frac{d\vec{V}}{dt} = -\nabla p + \rho g + \mu \ \nabla^2 \vec{V}
\end{aligned}
\tag{5.1.3}
$$

This equation is satisfied for laminar as well as turbulent flows and needs to be solved subjected to *no-slip* condition at the wall with known inlet/exit conditions. In the case of laminar flows, there are no random fluctuations and the shear stress terms are associated with the velocity gradients terms such as, $\mu \frac{\partial u}{\partial x}$, $\mu \frac{\partial u}{\partial y}$ and $\mu \frac{\partial u}{\partial z}$ in *x*-direction. For turbulent flows, velocity and pressure varies rapidly randomly as a function of space and time as shown in Fig. 5.1.3.

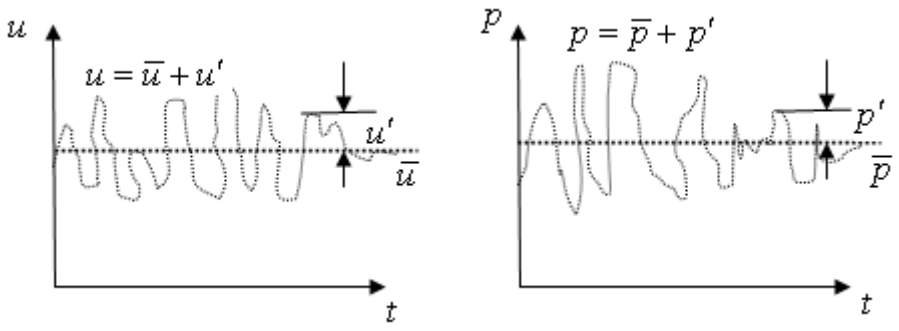

Fig. 5.1.3: Mean and fluctuating turbulent velocity and pressure.

One way to approach such problems is to define the mean/time averaged turbulent variables. The time mean of a turbulent velocity $(\bar{u})$ is defined by,

$$\bar{u} = \frac{1}{T}\int_0^T u\, dt \tag{5.1.4}$$

where, T is the averaging period taken as sufficiently longer than the period of fluctuations. If the fluctuation $u'(=u-\bar{u})$ is taken as the deviation from its average value, then it leads to zero mean value. However, the mean squared of fluctuation $\left(\overline{u'^2}\right)$ is not zero and thus is the measure of *turbulent intensity*.

$$\overline{u'} = \frac{1}{T}\int_0^T u'\, dt = \frac{1}{T}\int_0^T (u-\bar{u})\, dt = 0; \qquad \overline{u'^2} = \frac{1}{T}\int_0^T u'^2\, dt \neq 0 \tag{5.1.5}$$

In order to calculate the shear stresses in turbulent flow, it is necessary to know the fluctuating components of velocity. So, the *Reynolds time-averaging* concept is introduced where the velocity components and pressure are split into mean and fluctuating components;

$$u = \bar{u} + u';\ v = \bar{v} + v';\ w = \bar{w} + w';\ p = \bar{p} + p' \tag{5.1.6}$$

Substitute Eq. (5.1.6) in continuity equation (Eq. 5.1.3) and take time mean of each equation;

$$\frac{1}{T}\int_0^T\left(\frac{\partial \overline{u}}{\partial x}+\frac{\partial u'}{\partial x}\right)dt+\frac{1}{T}\int_0^T\left(\frac{\partial \overline{v}}{\partial y}+\frac{\partial v'}{\partial y}\right)dt+\frac{1}{T}\int_0^T\left(\frac{\partial \overline{w}}{\partial z}+\frac{\partial w'}{\partial z}\right)dt=0 \qquad (5.1.7)$$

Let us consider the first term of Eq. (4.1.7),

$$\frac{1}{T}\int_0^T\left(\frac{\partial \overline{u}}{\partial x}+\frac{\partial u'}{\partial x}\right)dt=\frac{1}{T}\left(\frac{\partial \overline{u}}{\partial x}\right)\int_0^T dt+\frac{1}{T}\frac{\partial}{\partial x}\int_0^T u'dt=\frac{\partial \overline{u}}{\partial x}+0=\frac{\partial \overline{u}}{\partial x} \qquad (5.1.8)$$

Considering the similar analogy for other terms, Eq. (5.1.7) is written as,

$$\frac{\partial \overline{u}}{\partial x}+\frac{\partial \overline{v}}{\partial y}+\frac{\partial \overline{w}}{\partial z}=0 \qquad (5.1.9)$$

This equation is very much similar with the continuity equation for laminar flow except the fact that the velocity components are replaced with the mean values of velocity components of turbulent flow. The momentum equation in *x*-direction takes the following form;

$$\rho\frac{d\overline{u}}{dt}=-\frac{\partial \overline{p}}{\partial x}+\rho g_x+\frac{\partial}{\partial x}\left(\mu\frac{\partial \overline{u}}{\partial x}-\rho\overline{u'^2}\right)+\frac{\partial}{\partial y}\left(\mu\frac{\partial \overline{u}}{\partial y}-\rho\overline{u'v'}\right)+\frac{\partial}{\partial z}\left(\mu\frac{\partial \overline{u}}{\partial z}-\rho\overline{u'w'}\right) \qquad (5.1.10)$$

The terms $-\rho\overline{u'^2}$, $-\rho\overline{u'v'}$ and $-\rho\overline{u'w'}$ in RHS of Eq. (5.1.3) have same dimensions as that of stress and called as *turbulent stresses*. For viscous flow in ducts and boundary layer flows, it has been observed that the stress terms associated with the *y*-direction (i.e. normal to the wall) is more dominant. So, necessary approximation can be made by neglecting other components of turbulent stresses and simplified expression may be obtained for Eq. (5.1.10).

$$\rho\frac{d\overline{u}}{dt}\approx-\frac{\partial \overline{p}}{\partial x}+\rho g_x+\frac{\partial \tau}{\partial y};\quad \tau=\mu\frac{\partial \overline{u}}{\partial y}-\rho\overline{u'v'}=\tau_{\text{lam}}+\tau_{\text{tur}} \qquad (5.1.11)$$

It may be noted that u' and v' are zero for laminar flows while the stress terms $-\rho\overline{u'v'}$ is positive for turbulent stresses. Hence the shear stresses in turbulent flow are always higher than laminar flow. The terms in the form of $-\rho\overline{u'v'}$, $-\rho\overline{v'w'}$, $-\rho\overline{u'w'}$ are also called as *Reynolds stresses*.

Turbulent velocity profile

A typical comparison of laminar and turbulent velocity profiles for wall turbulent flows, are shown in Fig. 5.1.4(a-b). The nature of the profile is parabolic in the case of laminar flow and the same trend is seen in the case of turbulent flow at the wall. The typical measurements across a turbulent flow near the wall have three distinct zones as shown in Fig. 5.1.4(c). The outer layer (τ_{tur}) is of two or three order magnitudes greater than the wall layer (τ_{lam}) and vice versa. Hence, the different sub-layers of Eq. (5.1.11) may be defined as follows;

- Wall layer (laminar shear dominates)
- Outer layer (turbulent shear dominates)
- Overlap layer (both types of shear are important)

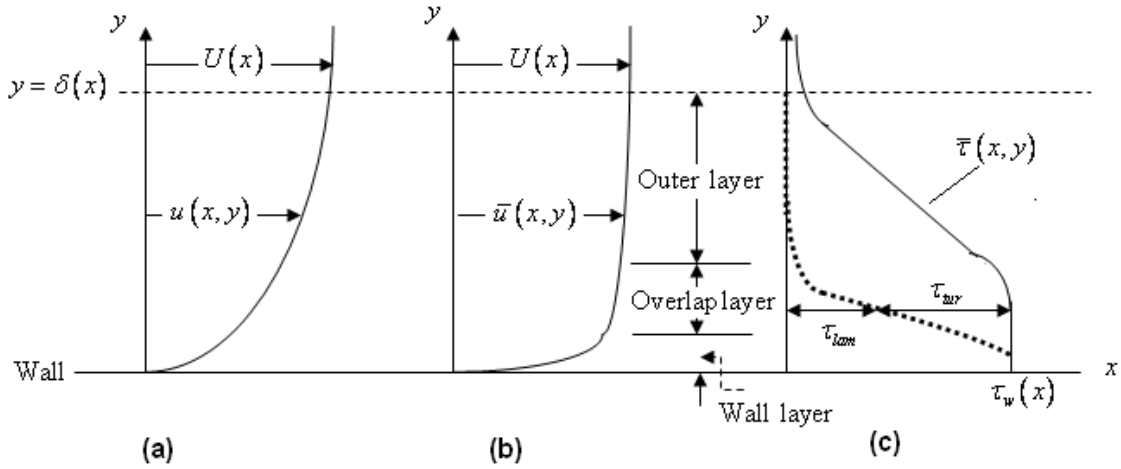

Fig 5.1.4: Velocity and shear layer distribution: (a) velocity profile in laminar flow; (b) velocity profile in turbulent flow; (c) shear layer in a turbulent flow.

In a typical turbulent flow, let the wall shear stress, thickness of outer layer and velocity at the edge of the outer layer be τ_w, δ and U, respectively. Then the velocity profiles (u) for different zones may be obtained from the empirical relations using dimensional analysis.

Wall layer: In this region, it is approximated that u is independent of shear layer thickness so that the following empirical relation holds good.

$$u = f\left(\mu, \tau_w, \rho, y\right);\ u^+ = \frac{u}{u^*} = F\left(\frac{y\rho u^*}{\mu}\right) \text{ and } u^* = \left(\frac{\tau_w}{\rho}\right)^{1/2} \tag{5.1.12}$$

Eq. (5.1.12) is known as the law of wall and the quantity u^* is called as friction velocity. It should not be confused with flow velocity.

Outer layer: The velocity profile in the outer layer is approximated as the deviation from the free stream velocity and represented by an equation called as *velocity-defect law*.

$$\left(U-u\right)_{outer} = g\left(\delta, \tau_w, \rho, y\right);\ \frac{U-u}{u^*} = G\left(\frac{y}{\delta}\right) \tag{5.1.13}$$

Overlap layer: Most of the experimental data show the very good validation of wall law and velocity defect law in the respective regions. An intermediate layer may be obtained when the velocity profiles described by Eqs. (5.1.12 & 5.1.13) overlap smoothly. It is shown that empirically that the overlap layer varies logarithmically with y (Eq. (5.1.14). This particular layer is known as *overlap layer*.

$$\frac{u}{u^*} = \frac{1}{0.41}\ln\left(\frac{y\rho u^*}{\mu}\right) + 5 \tag{5.1.14}$$

Module 5 : Lecture 2
VISCOUS INCOMPRESSIBLE FLOW
(Internal Flow – Part I)

Introduction

It has been discussed earlier that inviscid flows do not satisfy the *no-slip* condition. They slip at the wall but do not flow through wall. Because of complex nature of Navier-Stokes equation, there are practical difficulties in obtaining the analytical solutions of many viscous flow problems. Here, few classical cases of steady, laminar, viscous and incompressible flow will be considered for which the exact solution of Navier-Stokes equation is possible.

Viscous Incompressible Flow between Parallel Plates (Couette Flow)

Consider a two-dimensional incompressible, viscous, laminar flow between two parallel plates separated by certain distance $(2h)$ as shown in Fig. 5.2.1. The upper plate moves with constant velocity (V) while the lower is fixed and there is no pressure gradient. It is assumed that the plates are very wide and long so that the flow is essentially axial $(u \neq 0;\ v = w = 0)$. Further, the flow is considered far downstream from the entrance so that it can be treated as fully-developed.

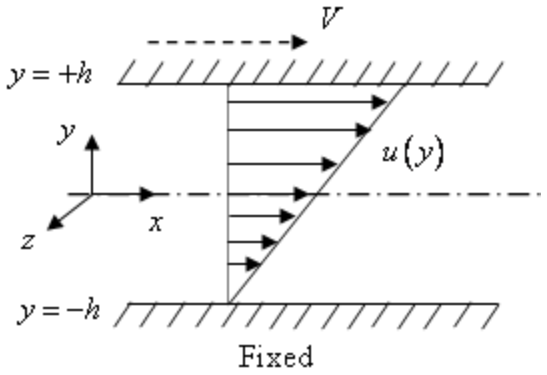

Fig. 5.2.1: Incompressible viscous flow between parallel plates with no pressure gradient.

The continuity equation is written as,

$$\frac{\partial u}{\partial x}+\frac{\partial v}{\partial y}+\frac{\partial w}{\partial z}=0;\ \Rightarrow\frac{\partial u}{\partial x}=0;\ \Rightarrow u=u\left(y\right)\text{ only} \tag{5.2.1}$$

As it is obvious from Eq. (5.2.1), that there is only a single non-zero velocity component that varies across the channel. So, only *x*-component of Navier-Stokes equation can be considered for this planner flow.

$$\begin{aligned}&\rho\left(u\frac{\partial u}{\partial x}+v\frac{\partial u}{\partial y}\right)=-\frac{\partial p}{\partial x}+\rho g_x+\mu\left(\frac{\partial^2 u}{\partial x^2}+\frac{\partial^2 u}{\partial y^2}\right)\\&\text{Since } u=u\left(y\right)\Rightarrow\frac{\partial u}{\partial x}=\frac{\partial^2 u}{\partial x^2}=0;\ v=0\\&\text{No pressure gradient }\Rightarrow\frac{\partial p}{\partial x}=0\\&\text{Gravity always acts vertically downward }\Rightarrow g_x=0\end{aligned} \tag{5.2.2}$$

Most of the terms in momentum equation drop out and Eq. (5.2.2) reduces to a second order ordinary differential equation. It can be integrated to obtain the solution of u as given below;

$$\frac{d^2u}{dy^2}=0\ \Rightarrow u=c_1y+c_2 \tag{5.2.3}$$

The two constants $\left(c_1\text{ and }c_2\right)$ can be obtained by applying no-slip condition at the upper and lower plates;

$$\begin{aligned}&\text{At } y=+h;\quad u=V=c_1h+c_2\\&\text{At } y=-h;\quad u=0=c_1\left(-h\right)+c_2\\&\Rightarrow c_1=\frac{V}{2h}\text{ and }c_2=\frac{V}{2}\end{aligned} \tag{5.2.4}$$

The solution for the flow between parallel plates is given below and plotted in Fig. 5.2.2 for different velocities of the upper plate.

$$\begin{aligned}&u=\left(\frac{V}{2h}\right)y+\frac{V}{2}\qquad -h\le y\le+h\\&\text{or, }\frac{u}{V}=\frac{1}{2}\left(1+\frac{y}{h}\right)\end{aligned} \tag{5.2.5}$$

It is a classical case where the flow is induced by the relative motion between two parallel plates for a viscous fluid and termed as *Coutte flow*. Here, the viscosity (μ) of the fluid does not play any role in the velocity profile. The shear stress at the wall (τ_w) can be found by differentiating Eq. (5.2.5) and using the following basic equation.

$$\tau_w = \mu \frac{du}{dy} = \frac{\mu V}{2h} \tag{5.2.6}$$

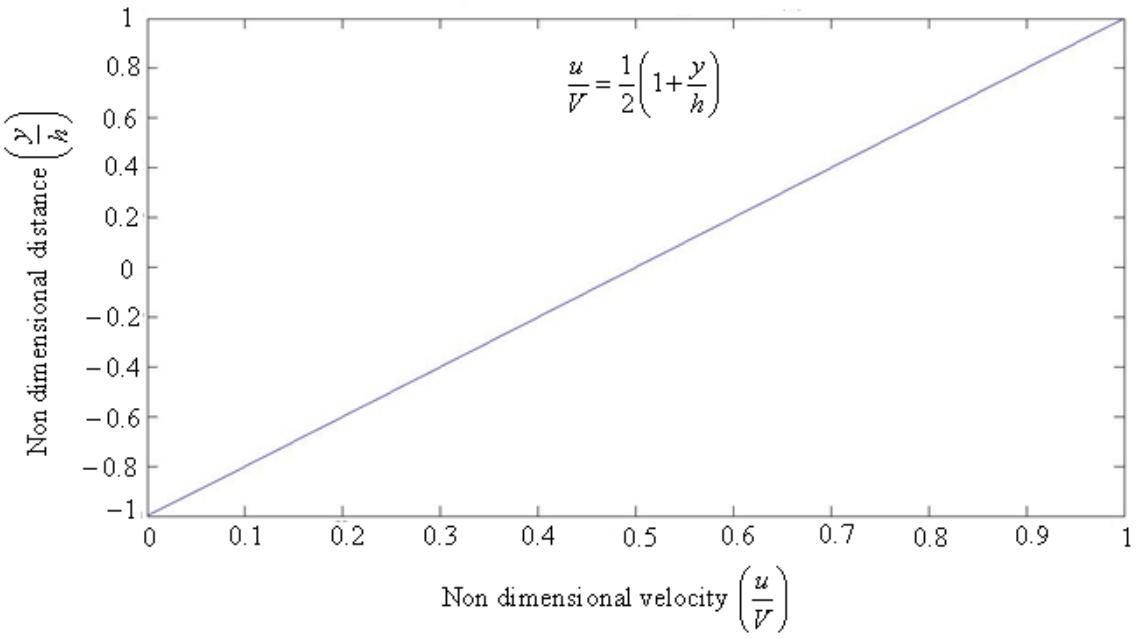

Fig. 5.2.2: Couette flow between parallel plates with no pressure gradient.

A typical application of *Couette flow* is found in the journal bearing where the main crankshaft rotates with an angular velocity (ω) and the outer one (i.e. housing) is a stationary member (Fig. 5.2.3). The gap width $(b = 2h = r_0 - r_i)$ is very small and contains lubrication oil.

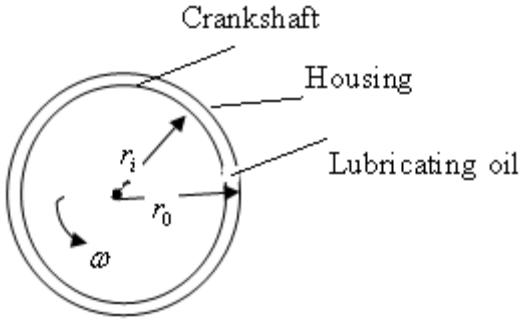

Fig. 5.2.3: Flow in a narrow gap of a journal bearing.

Since, $V = r_i \omega$, the velocity profile can be obtained from Eq. (5.2.5). The shearing stress resisting the rotation of the shaft can be simply calculated using Eq. (5.2.6).

$$\tau = \frac{\mu r_i \omega}{r_0 - r_i} \tag{5.2.7}$$

However, when the bearing is loaded (i.e. force is applied to the axis of rotation), the shaft will no longer remain concentric with the housing and the flow will no longer be parallel between the boundaries.

Viscous Incompressible Flow with Pressure Gradient (Poiseuille Flow)

Consider a two-dimensional incompressible, viscous, laminar flow between two parallel plates, separated by certain distance $(2h)$ as shown in Fig. 5.2.4. Here, both the plates are fixed but the pressure varies in *x*-direction. It is assumed that the plates are very wide and long so that the flow is essentially axial $(u \neq 0;\ v = w = 0)$. Further, the flow is considered far downstream from the entrance so that it can be treated as fully-developed. Using continuity equation, it leads to the same conclusion of Eq. (5.2.1) that $u = u(y)$ only. Also, $v = w = 0$ and gravity is neglected, the momentum equations in the respective direction reduces as follows;

$$\begin{aligned} &y-\text{momentum}: \frac{\partial p}{\partial y} = 0;\ \ z-\text{momentum}: \frac{\partial p}{\partial z} = 0 \ \ \Rightarrow p = p(x) \text{ only} \\ &x-\text{momentum}: \mu \frac{d^2 u}{dy^2} = \frac{\partial p}{\partial x} = \frac{dp}{dx} \end{aligned} \tag{5.2.8}$$

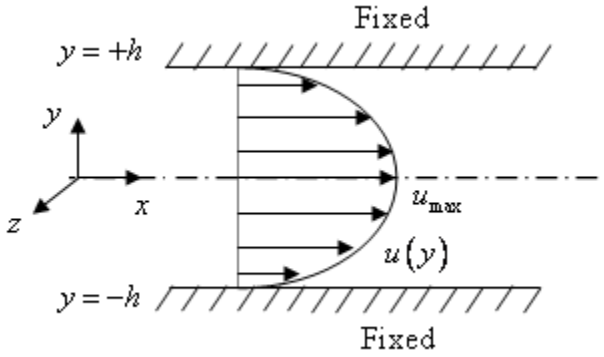

Fig. 5.2.4: Incompressible viscous flow between parallel plates with pressure gradient.

In the *x*-momentum equation, it may be noted that the left hand side contains the variation of u with y while the right hand side shows the variation of p with x. It must lead to a same constant otherwise they would not be independent to each other. Since the flow has to overcome the wall shear stress and the pressure must decrease in the direction of flow, the constant must be negative quantity. This type of pressure driven flow is called as *Poiseuille flow* which is very much common in the hydraulic systems, brakes in automobiles etc. The final form of equation obtained for a pressure gradient flow between two parallel fixed plates is given by,

$$\mu \frac{d^2u}{dy^2} = \frac{dp}{dx} = \text{constant} < 0 \tag{5.2.9}$$

The solution for Eq. (5.2.9) can be obtained by double integration;

$$u = \left(\frac{1}{\mu}\right)\left(\frac{dp}{dx}\right)\left(\frac{y^2}{2}\right) + c_3 y + c_4 \tag{5.2.10}$$

The constants can be found from *no-slip* condition at each wall:

$$\text{At } y = +h;\ u = 0 \Rightarrow c_1 = 0 \text{ and } c_2 = -\frac{dp}{dx}\left(\frac{h^2}{2\mu}\right) \tag{5.2.11}$$

After substitution of the constants, the general solution for Eq. (5.2.9) can be obtained;

$$u = -\left(\frac{dp}{dx}\right)\left(\frac{h^2}{2\mu}\right)\left(1 - \frac{y^2}{h^2}\right) \tag{5.2.12}$$

The flow described by Eq. (5.2.12) forms a *Poiseuille parabola* of constant curvature and the maximum velocity $\left(u_{\max}\right)$ occurs at the centerline $y = 0$:

$$u_{\max} = -\left(\frac{dp}{dx}\right)\left(\frac{h^2}{2\mu}\right) \tag{5.2.13}$$

The volume flow rate $\left(\dot{q}\right)$ passing between the plates (per unit depth) is calculated from the relationship as follows;,

$$\dot{q} = \int_{-h}^{h} u\, dy = \int_{-h}^{h} \left(\frac{1}{2\mu}\right)\left(\frac{dp}{dx}\right)\left(h^2 - y^2\right) dy = \frac{2h^3}{3\mu}\left(\frac{dp}{dx}\right) \tag{5.2.14}$$

If Δp represents the pressure-drop between two points at a distance l along x-direction, then Eq. (5.2.14) is expressed as,

$$\dot{q} = \frac{2h^3}{3\mu}\left(\frac{\Delta p}{l}\right) \tag{5.2.15}$$

The average velocity $\left(u_{avg}\right)$ can be calculated as follows;

$$u_{avg} = \frac{\dot{q}}{2h} = \frac{h^2}{3\mu}\left(\frac{\Delta p}{l}\right) = \left(\frac{3}{2}\right)u_{\max} \tag{5.2.16}$$

The wall shear stress for this case can also be obtained from the definition of Newtonian fluid;

$$\tau_w = \mu\left(\frac{\partial u}{\partial y} + \frac{\partial v}{\partial x}\right)_{y=\pm h} = \mu\frac{\partial}{\partial y}\left[\left(-\frac{dp}{dx}\right)\left(\frac{h^2}{2\mu}\right)\left(1-\frac{y^2}{h^2}\right)\right]_{y=\pm h} = \pm\left(\frac{dp}{dx}\right)h = \mp\frac{2\mu u_{\max}}{h} \tag{5.2.17}$$

The following silent features may be obtained from the analysis of *Couette and Poiseuille* flows;

- The *Couette* flow is induced by the relative motion between two parallel plates while the *Poiseuille* flow is a pressure driven flow.
- Both are planner flows and there is a non-zero velocity along *x*-direction while no velocity in *y and z* directions.
- The solutions for the both the flows are the exact solutions of Navier-Stokes equation.
- The velocity profile is linear for *Couette* flow with zero velocity at the lower plate with maximum velocity near to the upper plate.
- The velocity profile is parabolic for *Poiseuille* flow with zero velocity at the top and bottom plate with maximum velocity in the central line.
- In a *Poiseuille* flow, the volume flow rate is directly proportional to the pressure gradient and inversely related with the fluid viscosity.
- In a *Poiseuille* flow, the volume flow rate depends strongly on the cube of gap width.
- In a *Poiseuille* flow, the maximum velocity is 1.5-times the average velocity.

Module 5 : Lecture 3
VISCOUS INCOMPRESSIBLE FLOW
(Internal Flow – Part II)

Combined Couette - Poiseuille Flow between Parallel Plates

Another simple planner flow can be developed by imposing a pressure gradient between a fixed and moving plate as shown in Fig. 5.3.1. Let the upper plate moves with constant velocity (V) and a constant pressure gradient $\left(\frac{dp}{dx}\right)$ is maintained along the direction of the flow.

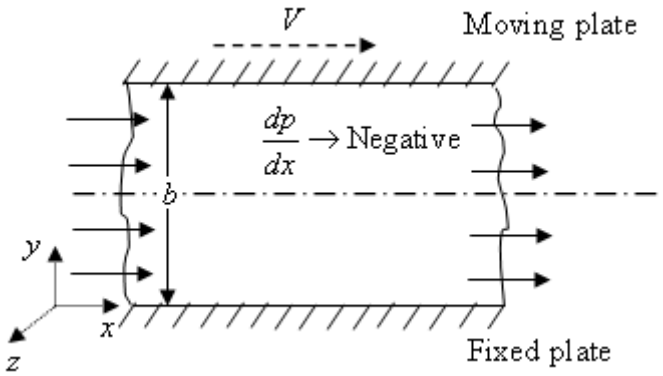

Fig. 5.3.1: Schematic representation of a combined *Couette-Poiseuille* flow.

The Navier-Stokes equation and its solution will be same as that of *Poiseuille* flow while the boundary conditions will change in this case;

$$\mu\frac{d^2u}{dy^2}=\frac{dp}{dx}=\text{constant}<0 \quad \text{and} \quad u=\left(\frac{1}{\mu}\right)\left(\frac{dp}{dx}\right)\left(\frac{y^2}{2}\right)+c_5y+c_6 \tag{5.3.1}$$

The constants can be found with two boundary conditions at the upper plate and lower plate;

$$\begin{aligned}&\text{At } y=0;\ u=0 \Rightarrow c_6=0\\ &\text{At } y=b;\ u=V \Rightarrow c_5=\frac{V}{b}-\left(\frac{b}{2\mu}\right)\left(\frac{dp}{dx}\right)\end{aligned} \tag{5.3.2}$$

After substitution of the constants, the general solution for Eq. (5.3.2) can be obtained;

$$\begin{aligned}&u=V\left(\frac{y}{b}\right)+\left(\frac{1}{2\mu}\right)\left(\frac{dp}{dx}\right)\left(y^2-by\right)\\ &\text{or, } \frac{u}{V}=\left(\frac{y}{b}\right)\left[1-\left(\frac{b^2}{2\mu V}\right)\left(\frac{dp}{dx}\right)\left(1-\frac{y}{b}\right)\right]\end{aligned} \tag{5.3.3}$$

The first part in the RHS of Eq. (5.3.3) is the solution for *Couette wall-driven flow* whereas the second part refers to the solution for *Poiseuille pressure-driven flow*. The actual velocity profile depends on the dimensionless parameter

$$P = \left(-\frac{b^2}{2\mu V} \right) \left(\frac{dp}{dx} \right) \tag{5.3.4}$$

Several velocity profiles can be drawn for different values of P as shown in Fig. 5.3.2. With $P = 0$, the simplest type of *Couette flow* is obtained with no pressure gradient. Negative values of P refers to *back flow* which means positive pressure gradient in the direction of flow.

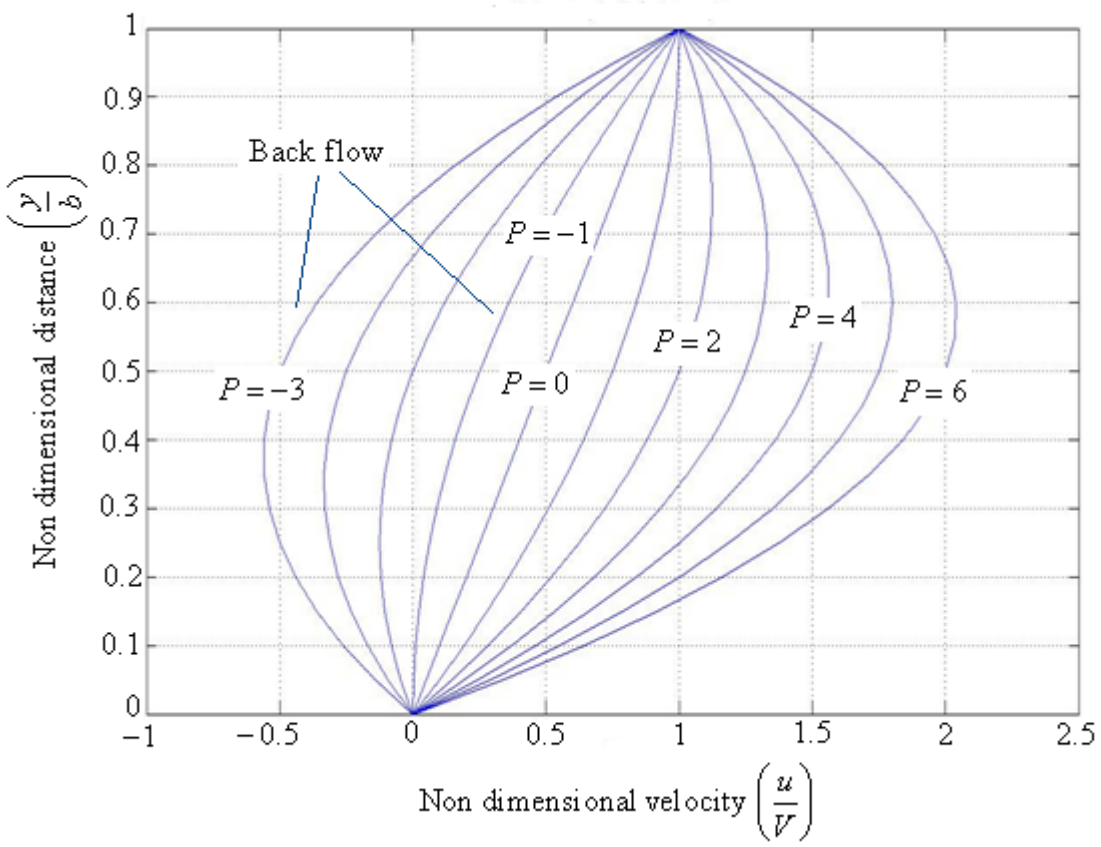

Fig. 5.3.2: Velocity profile for a combined *Couette-Poiseuille* flow between parallel plates.

Flow between Long Concentric Cylinders

Consider the flow in an annular space between two fixed, concentric cylinders as shown in Fig. 5.3.3. The fluid is having constant density and viscosity $(\mu \text{ and } \rho)$. The inner cylinder rotates at an angular velocity (ω_i) and the outer cylinder is fixed. There is no axial motion or end effects i.e. $v_z = 0$ and no change in velocity in the direction of θ i.e. $v_\theta = 0$. The inner and the outer cylinders have radii r_i and r_0, respectively and the velocity varies in the direction of r only.

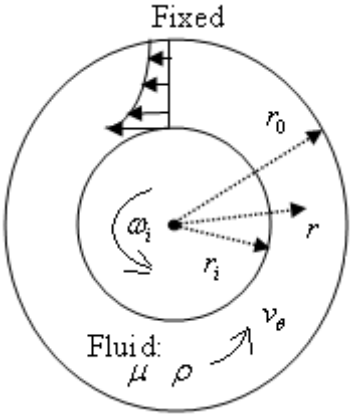

Fig. 5.3.3: Flow through an annulus.

The continuity and momentum equation may be written in cylindrical coordinates as follow;

$$\frac{1}{r}\frac{\partial(uv_r)}{\partial r}+\frac{1}{r}\frac{\partial v_\theta}{\partial \theta}=0;\ \Rightarrow \frac{1}{r}\frac{d(uv_r)}{dr}=0;\ \Rightarrow r\,v_r=\text{constant} \tag{5.3.5}$$

It is to be noted that v_θ does not vary with θ and at the inner and outer radii, there is no velocity. So, the motion can be treated as purely circumferential so that $v_r = 0$ and $v_\theta = v_\theta(r)$. The θ-momentum equation may be written as follows;

$$\rho\left(\vec{V}\cdot\nabla\right)v_\theta+\frac{\rho v_r v_\theta}{r}=-\frac{1}{r}\left(\frac{\partial p}{\partial \theta}\right)+\rho g_\theta+\mu\left(\nabla^2 v_\theta-\frac{v_\theta}{r^2}\right) \tag{5.3.6}$$

Considering the nature of the present problem, most of the terms in Eq. (5.3.6) will vanish except for the last term. Finally, the basic equation for the flow between rotating cylinders becomes a linear second-order ordinary differential equation.

$$\nabla^2 v_\theta=\frac{1}{r}\frac{d}{dr}\left(r\frac{dv_\theta}{dr}\right)=\frac{v_\theta}{r^2}\quad\Rightarrow v_\theta=c_1 r+\frac{c_2}{r} \tag{5.3.7}$$

The constants appearing in the solution of v_θ are found by no-slip conditions at the inner and outer cylinders;

$$\text{At } r = r_0;\ v_\theta = 0 = c_1 r_0 + \frac{c_2}{r_0} \quad \text{and} \quad \text{At } r = r_i;\ v_\theta = \omega_i r_i = c_1 r_i + \frac{c_2}{r_i}$$

$$\Rightarrow c_1 = \frac{\omega_i}{\left(1 - \frac{r_0^2}{r_i^2}\right)} \qquad \text{and} \quad c_2 = \frac{\omega_i}{\left(\frac{1}{r_i^2} - \frac{1}{r_0^2}\right)} \tag{5.3.8}$$

The final solution for velocity distribution is given by,

$$v_\theta = \omega_i r_i \left[\frac{(r_0/r) - (r/r_0)}{(r_0/r_i) - (r_i/r_0)}\right] \tag{5.3.9}$$

Module 5 : Lecture 4
VISCOUS INCOMPRESSIBLE FLOW
(Internal Flow – Part III)

Flow in a Circular pipe (Integral Analysis)

A classical example of a viscous incompressible flow includes the motion of a fluid in a closed conduit. It may be a *pipe* if the cross-section is round or *duct* if the conduit is having any other cross-section. The driving force for the flow may be due to the pressure gradient or gravity. In practical point of view, a *pipe/duct flow* (running in full) is driven mainly by *pressure* while an open channel flow is driven by gravity. However, the flow in a half-filled pipe having a free surface is also termed as *open channel flow*. In this section, only a fully developed laminar flow in a circular pipe is considered. Referring to geometry as shown in Fig. 5.4.1, the pipe having a radius (R) is inclined by an angle ϕ with the horizontal direction and the flow is considered in *x*-direction. The continuity relation for a steady incompressible flow in the control volume can be applied between section '1' and '2' for the constant area pipe (Fig. 5.4.1).

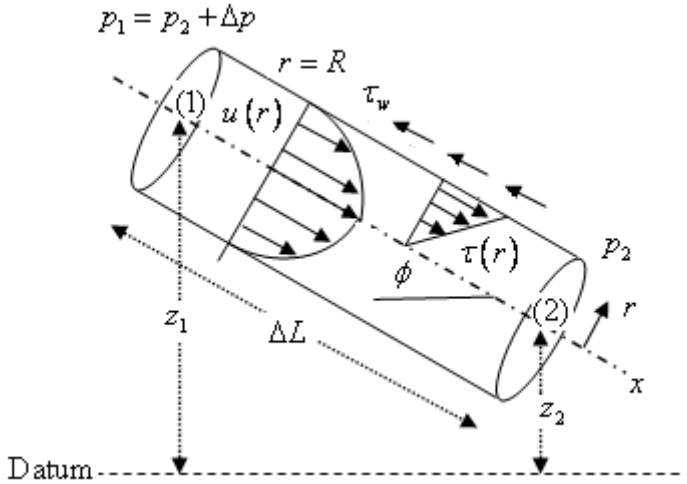

Fig. 5.4.1: Fully developed flow in an inclined pipe.

$$\int_{CS} \rho\left(\vec{V}.\vec{n}\right) dA = 0 \Rightarrow Q_1 = Q_2 = \text{constant} \Rightarrow u_{avg,1} = \frac{Q_1}{A_1} = u_{avg,2} = \frac{Q_2}{A_2} \qquad (5.4.1)$$

Neglect the entrance effect and assume a fully developed flow in the pipe. Since there is no shaft work or heat transfer effects, one can write the steady flow energy equation as,

$$\begin{aligned} &\frac{p_1}{\rho}+\frac{1}{2}u_{avg,1}^2+gz_1=\frac{p_2}{\rho}+\frac{1}{2}u_{avg,2}^2+gz_2+gh_f \\ &\text{or, } h_f=\left(z_1+\frac{p_1}{\rho g}\right)-\left(z_2+\frac{p_2}{\rho g}\right)=\Delta\left(z+\frac{p}{\rho g}\right)=\Delta z+\frac{\Delta p}{\rho g} \end{aligned} \tag{5.4.2}$$

Now recall the control volume momentum relation for the steady incompressible flow,

$$\sum\vec{F}=\sum\left(\dot{m}_i\vec{V}_i\right)_{out}-\sum\left(\dot{m}_i\vec{V}_i\right)_{in} \tag{5.4.3}$$

In the present case, LHS of Eq. (5.4.3) may be considered as pressure force, gravity and shear force.

$$\begin{aligned} &\Delta p\left(\pi R^2\right)+\rho g\left(\pi R^2\right)\Delta L\sin\phi-\tau_w\left(2\pi R\right)\Delta L=\dot{m}\left(V_1-V_2\right)=0 \\ &\text{or, } \Delta z+\frac{\Delta p}{\rho g}=h_f=\frac{2\tau_w}{\rho g}\left(\frac{\Delta L}{R}\right)\quad\left(\Delta z=\Delta L\sin\phi\right) \\ &\text{or, } \tau_w=\frac{R}{2}\left(\frac{\Delta p+\rho g\,\Delta z}{\Delta L}\right) \end{aligned} \tag{5.4.4}$$

Till now, no assumption is made, whether the flow is laminar or turbulent. It can be correlated to the shear stress on the wall $\left(\tau_w\right)$. In a general sense, the wall shear stress τ_w can be assumed to be the function of flow parameters such as, average velocity $\left(u_{avg}\right)$, fluid property$\left(\mu \text{ and } \rho\right)$, geometry$\left(d=2R\right)$ and quality $\left(\text{roughness } \varepsilon\right)$of the pipe.

$$\tau_w=F\left(\rho,\mu,u_{avg},d,\varepsilon\right) \tag{5.4.5}$$

By dimensional analysis, the following functional relationsip may be obtained;

$$\frac{8\tau_w}{\rho u_{avg}^2}=f=F\left(\mathrm{Re}_d,\frac{\varepsilon}{d}\right) \tag{5.4.6}$$

The desired expression for head loss in the pipe $\left(h_f\right)$ can be obtained by combining Eqs (5.4.4 & 5.4.6).

$$h_f=f\left(\frac{L}{d}\right)\frac{u_{avg}^2}{2g} \tag{5.4.7}$$

The dimensionless parameter f is called as *Darcy friction factor* and Eq. (5.4.7) is known as *Darcy-Weisbach equation*. This equation is valid for duct flow of any cross-section, irrespective of the fact whether the flow is laminar or turbulent. In the subsequent part of this module, it will be shown that, for duct flow of any cross-section the parameter d refers to equivalent diameter and the term (ε/d) vanishes for laminar flow.

Flow in a Circular Pipe (Differential Analysis)

Let us analyze the pressure driven flow (simply *Poiseuille flow*) through a straight circular pipe of constant cross section. Irrespective of the fact that the flow is laminar or turbulent, the continuity equation in the cylindrical coordinates is written as,

$$\frac{1}{r}\frac{\partial}{\partial r}(r v_r)+\frac{1}{r}\frac{\partial}{\partial \theta}(v_\theta)+\frac{\partial u}{\partial x}=0 \tag{5.4.8}$$

The important assumptions involved in the analysis are, *fully developed flow* so that $u=u(r)$ only and there is *no swirl or circumferential variation* i.e. $\left(v_\theta=0;\ \frac{\partial}{\partial \theta}=0\right)$ as shown in Fig. 5.4.1. So, Eq. (5.4.8) takes the following form;

$$\frac{1}{r}\frac{\partial}{\partial r}(r v_r)=0 \ \Rightarrow r v_r=\text{constant} \tag{5.4.9}$$

Referring to Fig. 5.4.1, *no-sip* conditions should be valid at the wall $(r=R;\ v_r=0)$. If Eq. (5.4.9) needs to be satisfied, then $v_r=0$, everywhere in the flow field. In other words, there is only one velocity component $u=u(r)$, in a fully developed flow. Moving further to the differential momentum equation in the cylindrical coordinates,

$$\rho u\frac{\partial u}{\partial x}=-\frac{dp}{dx}+\rho g_x+\frac{1}{r}\frac{\partial}{\partial r}(r\tau) \tag{5.4.10}$$

Since, $u=u(r)$, the LHS of Eq. (5.4.10) vanishes while the RHS of this equation is simplified with reference to the Fig. 5.4.1.

$$\frac{1}{r}\frac{\partial}{\partial r}(r\tau)=\frac{d}{dx}(p-\rho g\, x\sin\phi)=\frac{d}{dx}(p+\rho g\, z) \tag{5.4.11}$$

It is seen from Eq. (5.4.11) that LHS varies with r while RHS is a function of x. It must be satisfied if both sides have same constants. So, it can be integrated to obtain,

$$r\tau = \frac{r^2}{2}\left[\frac{d}{dx}\left(p + \rho g\, z\right)\right] + c \tag{5.4.12}$$

The constant of integration (c) must be zero to satisfy the condition of no shear stress along the center line $(r = 0;\ \tau = 0)$. So, the end result becomes,

$$\tau = \frac{r}{2}\left[\frac{d}{dx}\left(p + \rho g\, z\right)\right] = \text{constant}(r) \tag{5.4.13}$$

Further, at the wall the shear stress is represented as,

$$\tau_w = \frac{R}{2}\left(\frac{\Delta p + \rho g\, \Delta z}{\Delta L}\right) \tag{5.4.14}$$

It is seen that the shear stress varies linearly from centerline to the wall irrespective of the fact that the flow is laminar or turbulent. Further, when Eqs. (5.4.4 & 5.4.14) are compared, the wall shear stress is same in both the cases.

Laminar Flow Solutions

The exact solution of Navier-Stokes equation for the steady, incompressible, laminar flow through a circular pipe of constant cross-section is commonly known as *Hagen-Poiseuille* flow. Specifically, for laminar flow, the expression for shear stress (Eq. 5.4.13) can be represented in the following form;

$$\begin{aligned} &\tau = \mu\frac{du}{dr} = \frac{r}{2}K \quad \text{where } K = \frac{d}{dx}\left(p + \rho g\, z\right) = \text{constant} \\ &\Rightarrow u = \frac{r^2}{2}\left(\frac{K}{\mu}\right) + c_1 \end{aligned} \tag{5.4.15}$$

Eq. (5.4.15) can be integrated and the constant of integration is evaluated from no-slip condition, i.e. $\left(r=0;\ u=0\ \Rightarrow c_1=-R^2K/4\mu\right)$. After substituting the value of c_1, Eq. (5.4.15) can be simplified to obtain the laminar velocity profile for the flow through circular pipe which is commonly known as *Hagen-Poiseuille* flow. It resembles the nature of a paraboloid falling zero at the wall and maximum at the central line (Fig. 5.4.1 and Eq. 5.4.16).

$$\begin{aligned} u &= \frac{1}{4\mu}\left[-\frac{d}{dx}\left(p+\rho g\, z\right)\right]\left(R^2-r^2\right) \text{ and } u_{\max}=\frac{R^2}{4\mu}\left[-\frac{d}{dx}\left(p+\rho g\, z\right)\right] \\ \Rightarrow \frac{u}{u_{\max}} &= \left(1-\frac{r^2}{R^2}\right) \end{aligned} \tag{5.4.16}$$

The simplified form of velocity profile equation can be represented as below;

$$\frac{u}{u_{\max}}=\left(1-\frac{r^2}{R^2}\right) \tag{5.4.17}$$

Many a times, the pipe is horizontal so that $\Delta z=0$ and the other results such as volume flow rate $\left(Q\right)$ and average velocity $\left(u_{avg}\right)$ can easily be computed.

$$\begin{aligned} Q &= \int u\, dA=\int_0^R u_{\max}\left(1-\frac{r^2}{R^2}\right)\left(2\pi r\right)dr=\left(\frac{u_{\max}}{2}\right)\pi R^2=\frac{\pi R^4}{8\mu}\left(\frac{\Delta p}{L}\right) \\ \Rightarrow \Delta p &= \frac{8\mu L\ Q}{\pi R^4}=\frac{128\mu L\ Q}{\pi d^4}; \qquad u_{avg}=\frac{Q}{A}=\frac{Q}{\pi R^2}=\frac{u_{\max}}{2} \end{aligned} \tag{5.4.18}$$

The wall shear stress is obtained by evaluating the differential (Eq. 5.4.15) at the wall $r=R$ which is same as of Eq. (5.4.14)

$$\tau_w=\mu\left.\frac{du}{dr}\right|_{r=R}=\frac{2\mu u_{\max}}{R}=\frac{R}{2}\left|\frac{d}{dx}\left(p+\rho g\, z\right)\right|=\frac{R}{2}\left(\frac{\Delta p+\rho g\,\Delta z}{\Delta L}\right) \tag{5.4.19}$$

Referring to Eq. (5.4.6), the laminar friction factor can be calculated as,

$$f_{lam}=\frac{8\tau_w}{\rho u_{avg}^2}=\frac{8}{\rho u_{avg}^2}\frac{R}{2}\left[\frac{d}{dx}\left(p+\rho g\, z\right)\right]=\frac{8}{\rho u_{avg}^2}\frac{R}{2}\left(\frac{8\mu u_{avg}}{R^2}\right)=\frac{64\mu}{\rho u_{avg}d}=\frac{64}{\mathrm{Re}_d} \tag{5.4.20}$$

The laminar head loss is then obtained from Eq. (5.4.7) as below;

$$h_{f,lam}=\left(\frac{64\mu}{\rho u_{avg}d}\right)\left(\frac{L}{d}\right)\left(\frac{u_{avg}^2}{2g}\right)=\frac{32\mu L u_{avg}}{\rho g d^2}=\frac{128\mu LQ}{\pi\,\rho g d^4} \tag{5.4.21}$$

The following important inferences may be drawn from the above analysis;

- The nature of velocity profile in a laminar pipe flow is paraboloid with zero at the wall and maximum at the central-line.
- The maximum velocity in a laminar pipe flow is twice that of average velocity.
- In a laminar pipe flow, the friction factor drops with increase in flow Reynolds number.
- The shear stress varies linearly from center-line to the wall, being maximum at the wall and zero at the central-line. This is true for both laminar as well as turbulent flow.
- The wall shear stress is directly proportional to the maximum velocity and independent of density because the fluid acceleration is zero.
- For a certain fluid with given flow rate, the laminar head loss in a pipe flow is directly proportional to the length of the pipe and inversely proportional to the fourth power of pipe diameter.

Module 5 : Lecture 5
VISCOUS INCOMPRESSIBLE FLOW
(Internal Flow – Part IV)

Turbulent Flow through Pipes

The flows are generally classified as laminar or turbulent and the turbulent flow is more prevalent in nature. It is generally observed that the turbulence in the flow field can change the mean values of any important parameter. For any geometry, the flow Reynolds number is the parameter that decides if there is any change in the nature of the flow i.e. laminar or turbulent. An experimental evidence of transition was reported first by German engineer *G.H.L Hagen* in the year 1830 by measuring the pressure drop for the water flow in a smooth pipe (Fig. 5.5.1).

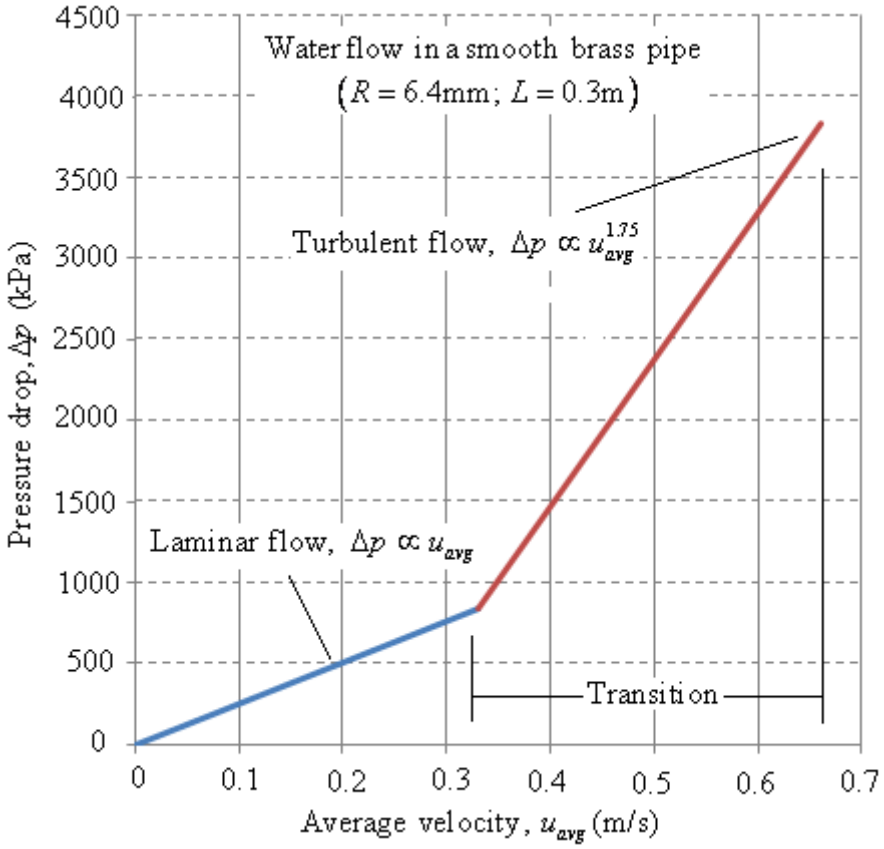

Fig. 5.5.1: Experimental evidence of transition for water flow in a brass pipe (*Re-plotted using the data given in White 2003*)

The approximate relationship follows the pressure drop (Δp) law as given in the following equation;

$$\Delta p = \frac{\mu L Q}{R^4} + E_f \tag{5.5.1}$$

where, E_f is the entrance effect in terms of pressure drop, μ is the fluid viscosity, Q is the volume flow, L and R are the length and radius of the pipe, respectively. It is seen from Fig. (5.5.1) that the pressure drop varies linearly with velocity up to the value 0.33m/s and a sharp change in pressure drop is observed after the velocity is increased above 0.6m/s. During the velocity range of 0.33 to 0.6m/s, the flow is treated to be under transition stage. When such a transition takes place, it is normally initiated through turbulent *spots/bursts* that slowly disappear as shown in Fig. 5.5.2. In the case of pipe flow, the flow Reynolds number based on pipe diameter is above 2100 for which the transition is noticed. The flow becomes entirely turbulent if the Reynolds number exceeds 4000.

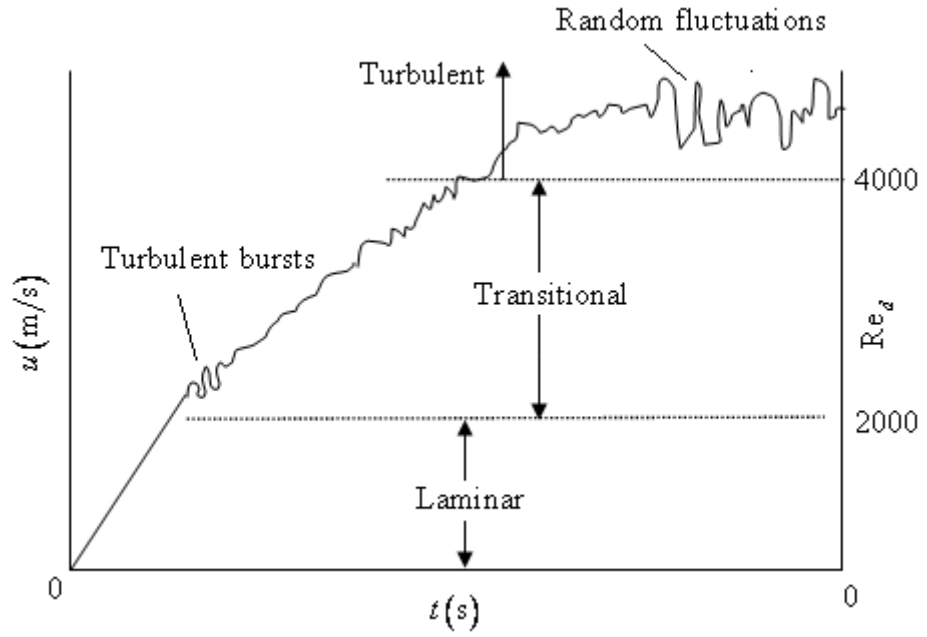

Fig. 5.5.2: Schematic representation of laminar to turbulent transition in a pipe flow.

Turbulent Flow Solutions

In the case of turbulent flow, one needs to rely on the empirical relations for velocity profile obtained from *logarithmic law*. If $u(r)$ is the local mean velocity across the pipe of radius R and $u^*\left(=\sqrt{\frac{\tau_w}{\rho}}\right)$ is the *friction velocity*, then the following empirical relation holds good;

$$\frac{u}{u^*} \approx \frac{1}{\kappa}\ln\frac{(R-r)\rho u^*}{\mu} + B \tag{5.5.2}$$

The average velocity (u_{avg}) for this profile can be computed as,

$$u_{avg} = \frac{Q}{A} = \frac{1}{\pi R^2}\int_0^R u^*\left[\frac{1}{\kappa}\ln\frac{(R-r)\rho u^*}{\mu} + B\right](2\pi R)\,dr = \frac{1}{2}u^*\left(\frac{2}{\kappa}\ln\frac{R\rho u^*}{\mu} + 2B - \frac{3}{\kappa}\right) \tag{5.5.3}$$

Using the approximate values of $\kappa = 0.41$ and $B = 5$, the simplified relation for turbulent velocity profile is obtained as below;

$$\frac{u_{avg}}{u^*} \approx 2.44\ln\left(\frac{R\rho u^*}{\mu}\right) + 1.34 \tag{5.5.4}$$

Recall the *Darcy friction factor* which relates the wall shear stress (τ_w) and average velocity (u_{avg});

$$f = \frac{8\tau_w}{\rho u_{avg}^2} \quad \Rightarrow u_{avg} = \left(\frac{8\tau_w}{\rho f}\right)^{1/2} = u^*\left(\frac{8}{f}\right)^{1/2} \Rightarrow \frac{u_{avg}}{u^*} = \left(\frac{8}{f}\right)^{1/2} \tag{5.5.5}$$

Rearrange the first term appearing in RHS of Eq. (5.5.4)

$$\frac{R\rho u^*}{\mu} = \frac{(1/2)\,d\,u_{avg}\,\rho}{\mu}\left(\frac{u^*}{u_{avg}}\right) = \frac{1}{2}\mathrm{Re}_d\left(\frac{f}{8}\right)^{1/2} \tag{5.5.6}$$

Substituting Eqs. (5.5.5 & 5.5.6) in Eq. (5.5.4) and simplifying, one can get the following relation for friction factor for the turbulent pipe flow.

$$\frac{1}{f^{0.5}} \approx 1.99\log\left(\mathrm{Re}_d\, f^{0.5}\right) - 1.02 \tag{5.5.7}$$

Since, Eq. (5.5.7) is implicit in nature, it becomes cumbersome to obtain friction factor for a given Reynolds number. So, there are many alternative explicit approximations as given below;

$$\begin{aligned} f &= 0.316\left(\mathrm{Re}_d\right)^{-0.25} \quad 4000 < \mathrm{Re}_d < 10^5 \\ &= \left(1.8\log\frac{\mathrm{Re}_d}{6.9}\right)^{-2} \end{aligned} \tag{5.5.8}$$

Further, the maximum velocity in the turbulent pipe flow is obtained from (5.5.2) and is evaluated at $r = 0$;

$$\frac{u_{\max}}{u^*} \approx \frac{1}{\kappa}\ln\frac{R\rho u^*}{\mu} + B \tag{5.5.9}$$

Another correlation may be obtained by relating Eq. (5.5.9) with the average velocity (Eq. 5.5.3);

$$\frac{u_{avg}}{u_{\max}} \approx \left(1+1.33\sqrt{f}\right)^{-1} \tag{5.5.10}$$

For a horizontal pipe at low Reynolds number, the head loss due to friction can be obtained from pressure drop as shown below;

$$\begin{aligned} h_{f,tur} = \frac{\Delta p}{\rho g} &= f\left(\frac{L}{d}\right)\left(\frac{u_{avg}^2}{2g}\right) \approx 0.316\left(\frac{\mu}{\rho u_{avg} d}\right)^{0.25}\left(\frac{L}{d}\right)\left(\frac{u_{avg}^2}{2g}\right) \\ &\approx 0.316\left(\frac{1}{\mathrm{Re}_d}\right)^{0.25}\left(\frac{L}{d}\right)\left(\frac{u_{avg}^2}{2g}\right) \end{aligned} \tag{5.5.11}$$

Simplifying Eq. (5.4.11), the pressure drop in a turbulent pipe flow may be expressed in terms of average velocity or flow rate;

$$\Delta p \approx 0.158\, L\,\rho^{0.75}\mu^{0.25}d^{-1.25}u_{avg}^{1.75} \approx 0.241\, L\,\rho^{0.75}\mu^{0.25}d^{-4.75}Q^{1.75} \tag{5.5.12}$$

For a given pipe, the pressure drop increases with average velocity power of 1.75 (Fig. 5.5.1) and varies slightly with the viscosity which is the characteristics of a turbulent flow. Again for a given flow rate, the turbulent pressure drop decreases with diameter more sharply than the laminar flow formula. Hence, the simplest way to reduce the pumping pressure is to increase the size of the pipe although the larger pipe is more expensive.

Moody Chart

The *surface roughness* is one of the important parameter for initiating transition in a flow. However, its effect is negligible if the flow is laminar but a turbulent flow is strongly affected by roughness. The surface roughness is related to frictional resistance by a parameter called as roughness ratio (ε/d), where ε is the roughness height and d is the diameter of the pipe. The experimental evidence show that friction factor (f) becomes constant at high Reynolds number for any given roughness ratio (Fig. 5.5.3). Since a turbulent boundary layer has three distinct regions, the friction factor becomes more dominant at low/moderate Reynolds numbers. So another dimensionless parameter $\varepsilon^+ \left(= \frac{\varepsilon u^* \rho}{\mu} \right)$, is defined that essentially show the effects of surface roughness on friction at low/moderate Reynolds number. In a hydraulically smooth wall, there is no effect of roughness on friction and for a fully rough flow, the sub-layer is broken and friction becomes independent of Reynolds number.

$\varepsilon^+ < 5$: Hydraulically smooth wall
$5 < \varepsilon^+ < 70$: Transitional roughness
$\varepsilon^+ > 70$: Fully rough flow

The dependence of friction factor on roughness ratio and Reynolds number for a turbulent pipe flow is represented by *Moody chart*. It is an accepted design formula for turbulent pipe friction within an accuracy of ±15% and based on the following empirical relations;

$$\frac{1}{f^{0.5}} = -2\log\left(\frac{\varepsilon/d}{3.7} + \frac{2.51}{\mathrm{Re}_d\, f^{0.5}}\right); \quad \frac{1}{f^{0.5}} = -1.8\log\left[\left(\frac{\varepsilon/d}{3.7}\right)^{1.11} + \frac{6.9}{\mathrm{Re}_d}\right] \tag{5.5.13}$$

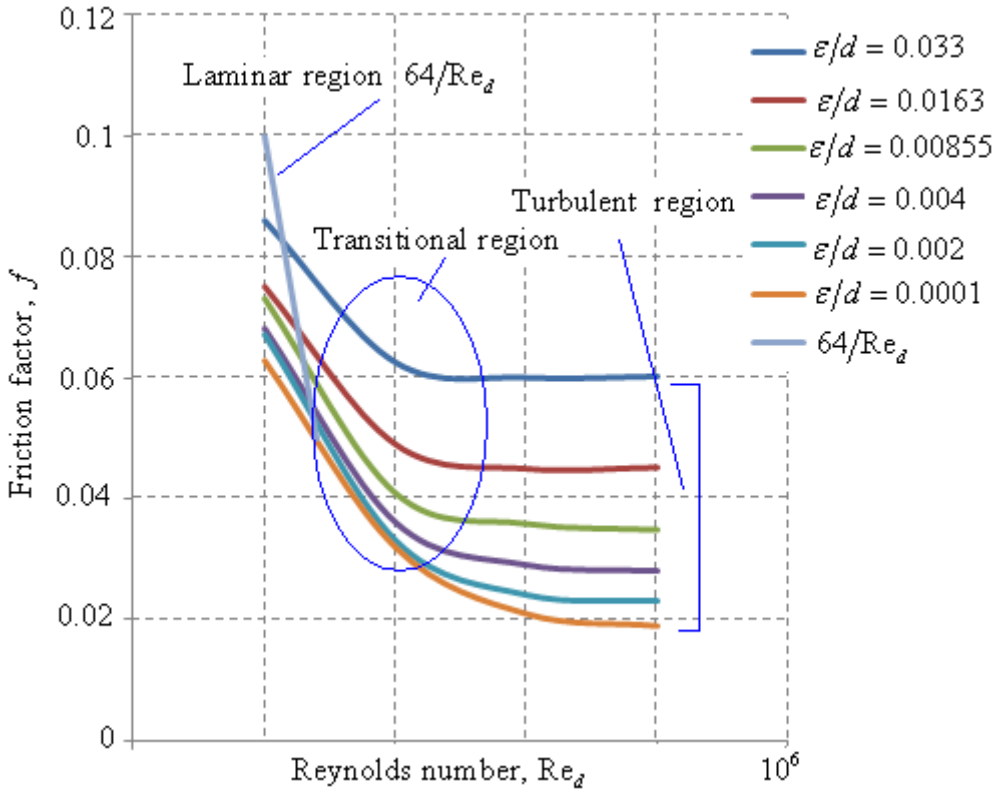

Fig. 5.5.3: Effect of wall roughness on turbulent pipe flow.
(*Re-plotted using the data given in White 2003*)

Module 5 : Lecture 6
VISCOUS INCOMPRESSIBLE FLOW
(Internal Flow – Part V)

Non-Circular Ducts and Hydraulic Diameter

The analysis of fully-developed flow (laminar/turbulent) in a non-circular duct is more complicated algebraically. The concept of *hydraulic diameter* is a reasonable method by which one can correlate the laminar/turbulent fully-developed pipe flow solutions to obtain approximate solutions of non-circular ducts. As derived from momentum equation in previous section, the head loss $\left(h_f\right)$ for a pipe and the wall shear stress $\left(\tau_w\right)$ is related as,

$$h_f = f\left(\frac{L}{d}\right)\left(\frac{u_{avg}^2}{2g}\right) = \frac{2\tau_w}{\rho g}\frac{\Delta L}{R} \tag{5.6.1}$$

The analogous form of same equation for a non-circular duct is written as,

$$h_f = \frac{2\overline{\tau}_w}{\rho g}\frac{\Delta L}{\left(A/P_e\right)} \tag{5.6.2}$$

where, $\overline{\tau}_w$ is the average shear stress integrated around the perimeter of the non-circular duct $\left(P_e\right)$ so that the ratio of cross-sectional area $\left(A\right)$ and the perimeter takes the form of length scale similar to the pipe radius $\left(R\right)$. So, the hydraulic radius $\left(R_h\right)$ of a non-circular duct is defined as,

$$R_h = \frac{A}{P_e} = \frac{\text{Cross-sectional area}}{\text{Wetted perimeter}} \tag{5.6.3}$$

If the cross-section is circular, the hydraulic diameter can be obtained from Eq. (5.6.3) as, $d_h = 4R_h$. So, the corresponding parameters such as friction factor and head loss for non-circular ducts (NCD) are then written as,

$$f_{NCD} = \frac{8\overline{\tau}_w}{\rho u_{avg}^2};\ h_f = f_{NCD}\left(\frac{L}{4R_h}\right)\frac{u_{avg}^2}{2g} \tag{5.6.4}$$

It is to be noted that the wetted perimeter includes all the surfaces acted upon by the shear stress. While finding the laminar/turbulent solutions of non-circular ducts, one must replace the radius/diameter of pipe flow solutions with the length scale term of hydraulic radius/diameter.

Minor Losses in Pipe Systems

The fluid in a typical piping system consists of inlets, exits, enlargements, contractions, various fittings, bends and elbows etc. These components interrupt the smooth flow of fluid and cause additional losses because of mixing and flow separation. So in typical systems with long pipes, the total losses involve the *major losses* (head loss contribution) and the *minor losses* (any other losses except head loss). The major head losses for laminar and turbulent pipe flows have already been discussed while the cause of additional minor losses may be due to the followings;

- Pipe entrance or exit
- Sudden expansion or contraction
- Gradual expansion or contraction
- Losses due to pipe fittings (valves, bends, elbows etc.)

A desirable method to express minor losses is to introduce an equivalent length $\left(L_{eq}\right)$ of a straight pipe that satisfies *Darcy friction-factor* relation in the following form;

$$h_m = f\left(\frac{L_{eq}}{d}\right)\left(\frac{u_{avg}^2}{2g}\right) = K_m\left(\frac{u_{avg}^2}{2g}\right);\quad L_{eq} = \frac{K_m d}{f} \tag{5.6.5}$$

where, K_m is the minor loss coefficient resulting from any of the above sources. So the total loss coefficient for a constant diameter $\left(d\right)$ pipe is given by the following expression;

$$\Delta h_{total} = h_f + \sum h_m = \left(\frac{u_{avg}^2}{2g}\right)\left(\frac{f\,L}{d} + \sum K_m\right) \tag{5.6.6}$$

It should be noted from Eq. (5.6.6) that the losses must be added separately if the pipe size and the average velocity for each component change. The total length $\left(L\right)$ is considered along the pipe axis including any bends.

Entrance and Exit Losses: Any fluid from a reservoir may enter into the pipe through variety of shaped region such as re-entrant, square-edged inlet and rounded inlet. Each of the geometries shown in Fig. 5.6.1 is associated with a minor head loss coefficient $\left(K_m\right)$. A typical flow pattern (Fig. 5.6.2) of a square-edged entrance region has a *vena-contracta* because the fluid cannot turn at right angle and it must separate from the sharp corner. The maximum velocity at the section (2) is greater than that of section (3) while the pressure is lower. Had the flow been slowed down efficiently, the kinetic energy could have converted into pressure and an ideal pressure distribution would result as shown through dotted line (Fig. 5.6.2). An obvious way to reduce the entrance loss is to rounded entrance region and thereby reducing the *vena-contracta* effect.

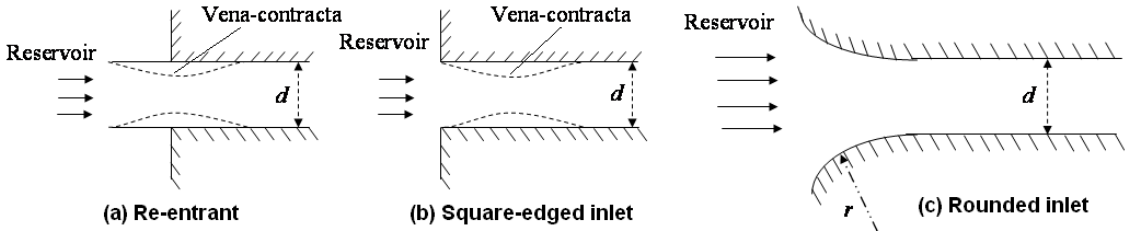

Fig. 5.6.1: Typical inlets for entrance loss in a pipe: (a) Reentrant $\left(K_m = 0.8\right)$**; (b) Sharp-edged inlet** $\left(K_m = 0.5\right)$**; (c) Rounded inlet** $\left(K_m = 0.04\right)$.

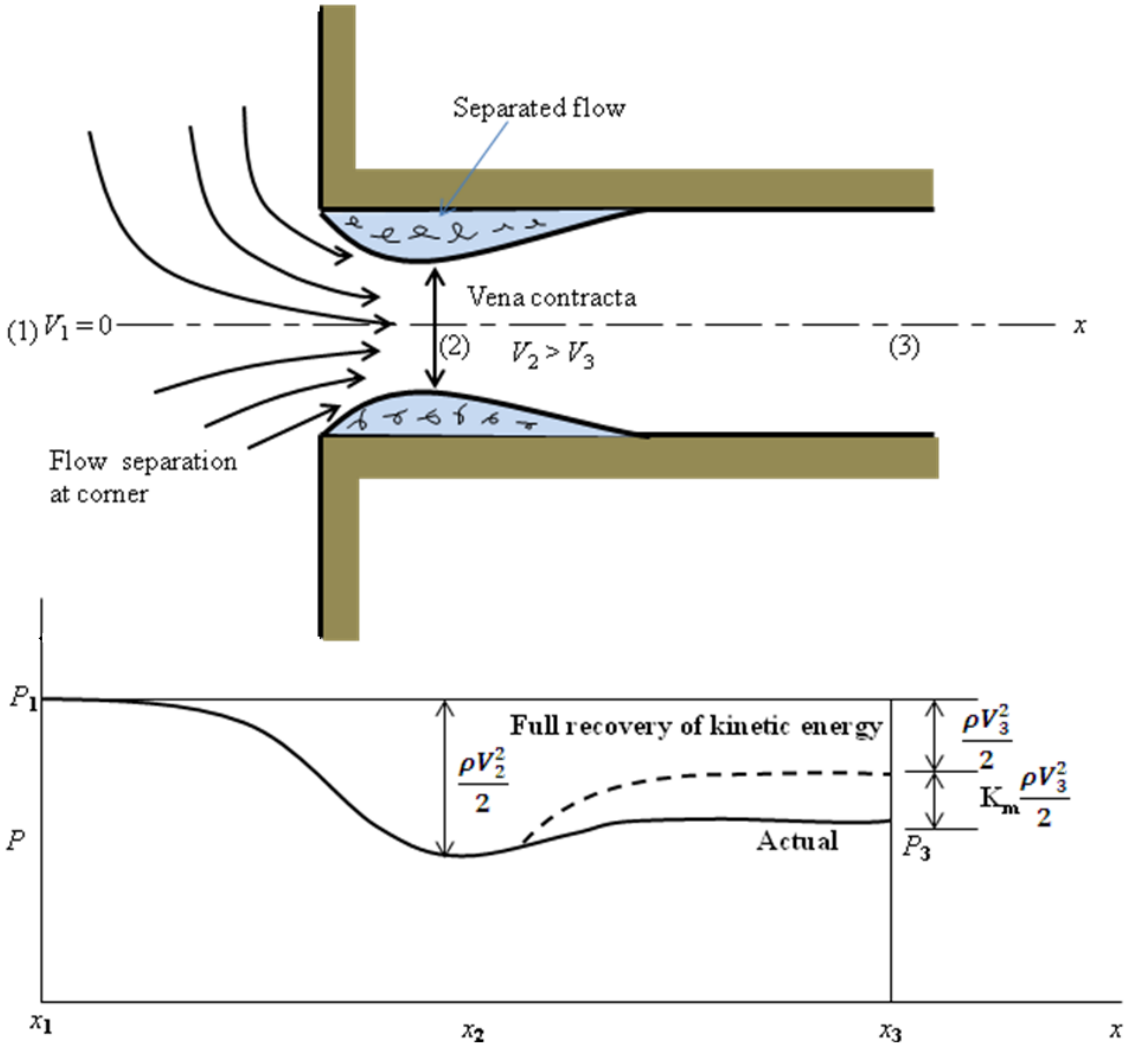

Fig. 5.6.2: Flow pattern for sharp-edged entrance.

The minor head loss is also produced when the fluid flows through these geometries enter into the reservoir (Fig. 5.6.1). These losses are known as exit losses. In these cases, the flow simply passes out of the pipe into the large downstream reservoir, loses its entire velocity head due to viscous dissipation and eventually comes to rest. So, the minor exit loss is equivalent to one velocity head $(K_m = 1)$, no matter how well the geometry is rounded.

Sudden Expansion and Contraction: The minor losses also appear when the flow through the pipe takes place from a larger diameter to the smaller one or vice versa. In the case of sudden expansion, the fluid leaving from the smaller pipe forms a jet initially in the larger diameter pipe, subsequently dispersed across the pipe and a fully-developed flow region is established (Fig. 5.6.3). In this process, a portion of the kinetic energy is dissipated as a result of viscous effects with a limiting case $(A_1/A_2)=0$.

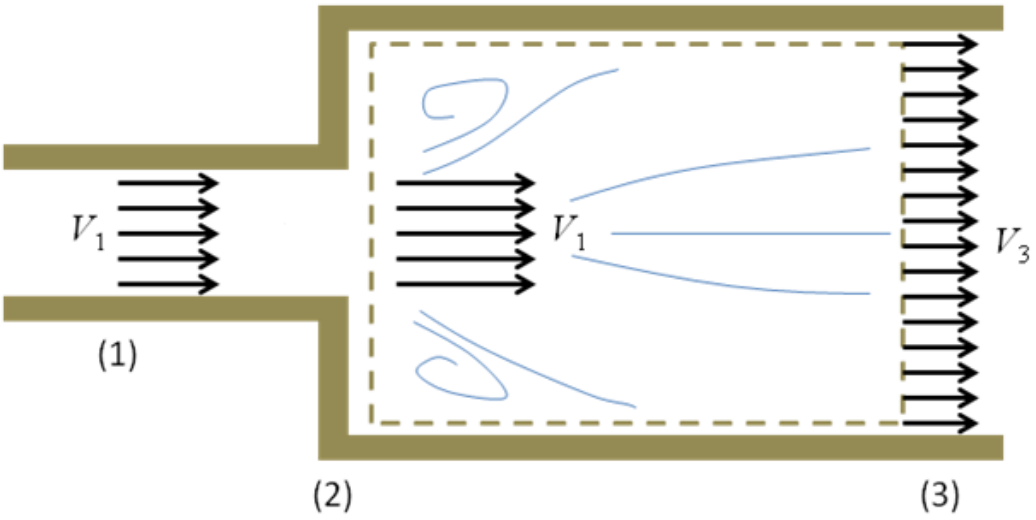

Fig. 5.6.3: Flow pattern during sudden expansion.

The loss coefficient during sudden expansion can be obtained by writing control volume continuity and momentum equation as shown in Fig. 5.6.3. Further the energy equation is applied between the sections (2) and (3). The resulting governing equations are written as follows;

$$\begin{aligned}&\text{Continuity}: \ A_1 V_1 = A_2 V_2 \\ &\text{Momentum}: \ p_1 A_3 - p_3 A_3 = \rho A_3 V_3 (V_3 - V_1) \\ &\text{Energy}: \frac{p_1}{\rho g} + \frac{V_1^2}{2g} = \frac{p_3}{\rho g} + \frac{V_3^2}{2g} + h_m\end{aligned} \qquad (5.6.7)$$

The terms in the above equation can be rearranged to obtain the loss coefficient as given below;

$$K_m = \frac{h_m}{\left(V_1^2/2g\right)} = \left(1 - \frac{A_1}{A_2}\right)^2 = \left(1 - \frac{d^2}{D^2}\right)^2 \qquad (5.6.8)$$

Here, A_1 and A_2 are the cross-sectional areas of small pipe and larger pipe, respectively. Similarly, d and D are the diameters of small and larger pipe, respectively.

For the case of sudden contraction, the flow initiates from a larger pipe and enters into the smaller pipe (Fig. 5.6.4). The flow separation in the downstream pipe causes the main stream to contract through minimum diameter $\left(d_{\min}\right)$, called as *vena-contracta*. This is similar to the case as shown in Fig. 5.6.2. The value of minor loss coefficient changes gradually (Fig. 5.6.5) from one extreme with $K_m = 0.5$ at $\left(A_1/A_2\right) = 0$ to the other extreme of $K_m = 0$ at $\left(A_1/A_2\right) = 1$. Another empirical relation for minor loss coefficient during sudden contraction is obtained through experimental evidence (Eq. 5.6.9) and it holds good with reasonable accuracy in many practical situations.

$$K_m \approx 0.42\left(1 - \frac{d^2}{D^2}\right) \tag{5.6.9}$$

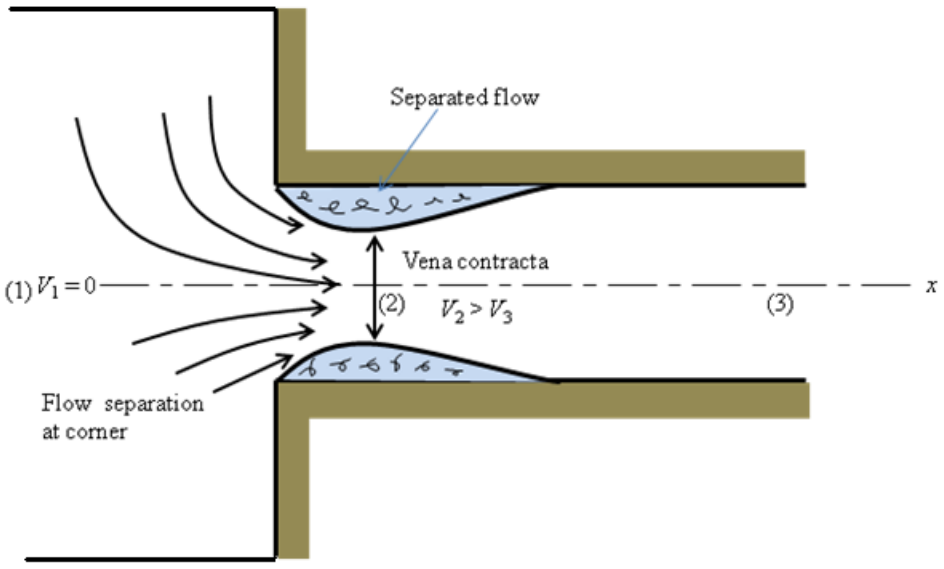

Fig. 5.6.4: Flow pattern during sudden contraction.

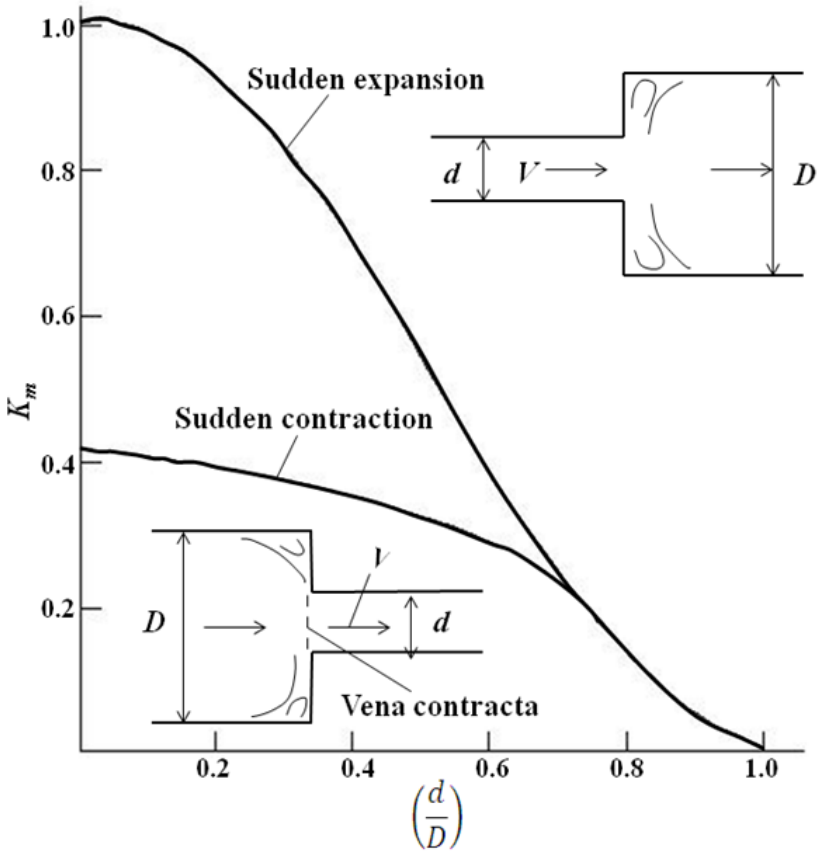

Fig. 5.6.5: Variation of loss coefficient with area ratio in a pipe.

Gradual Expansion and Contraction: If the expansion or contraction is gradual, the losses are quite different. A gradual expansion situation is encountered in the case of a diffuser as shown in Fig. 5.6.6. A diffuser is intended to raise the static pressure of the flow and the extent to which the pressure is recovered, is defined by the parameter pressure-recovery coefficient $\left(C_p\right)$. The loss coefficient is then related to this parameter C_p. For a given area ratio, the higher value of C_p implies lower loss coefficient K_m.

$$C_p = \frac{p_2 - p_1}{(1/2)\rho V_1^2}; \quad K_m = \frac{h_m}{V_1^2/(2g)} = 1 - \left(\frac{d_1}{d_2}\right)^4 - C_p \tag{5.6.10}$$

When the contraction is gradual, the loss coefficients based on downstream velocities are very small. The typical values of K_m range from 0.02 – 0.07 when the included angle changes from 30º to 60º. Thus, it is relatively easy to accelerate the fluid efficiently.

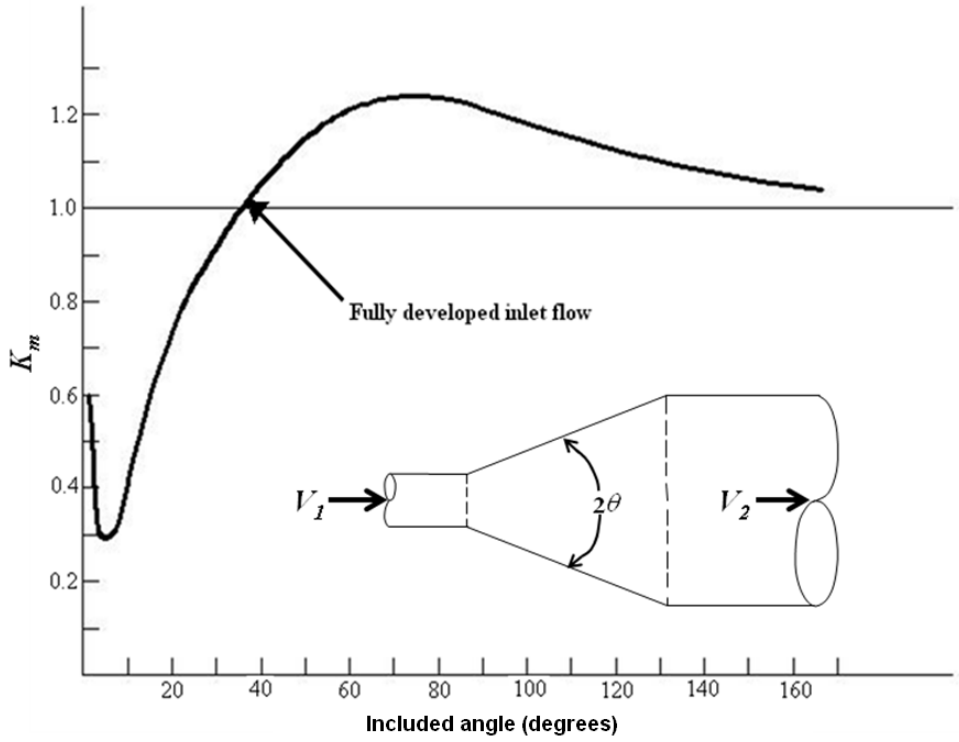

Fig. 5.6.6: Loss coefficients for gradual expansion and contraction.

Minor losses due to pipe fittings: A piping system components normally consists of various types of fitting such as valves, elbows, tees, bends, joints etc. The loss coefficients in these cases strongly depend on the shape of the components. Many a times, the value of K_m is generally supplied by the manufacturers. The typical values may be found in any reference books.

Module 5 : Lecture 7
VISCOUS INCOMPRESSIBLE FLOW
(External Flow – Part I)

General Characteristics of External Flow

External flows are defined as the flows immersed in an unbounded fluid. A body immersed in a fluid experiences a resultant force due to the interaction between the body and fluid surroundings. In some cases, the body moves in stationary fluid medium (e.g. motion of an airplane) while in some instances, the fluid passes over a stationary object (e.g. motion of air over a model in a wind tunnel). In any case, one can fix the coordinate system in the body and treat the situation as the flow past a stationary body at a uniform velocity (U), known as upstream/free-stream velocity. However, there are unusual instances where the flow is not uniform. Even, the flow in the vicinity of the object can be unsteady in the case of a steady, uniform upstream flow. For instances, when wind blows over a tall building, different velocities are felt at top and bottom part of the building. But, the unsteadiness and non-uniformity are of minor importance rather the flow characteristic on the surface of the body is more important. The shape of the body (e.g. sharp-tip, blunt or streamline) affects structure of an external flow. For analysis point of view, the bodies are often classified as, two-dimensional objects (infinitely long and constant cross-section), axi-symmetric bodies and three-dimensional objects.

There are a number of interesting phenomena that occur in an external viscous flow past an object. For a given shape of the object, the characteristics of the flow depend very strongly on carious parameters such as size, orientation, speed and fluid properties. The most important dimensionless parameter for a typical external incompressible flow is the Reynolds number $\left(\mathrm{Re} = \frac{\rho U l}{\mu}\right)$, which represents the ratio of inertial effects to the viscous effects. In the absence of viscous effects $(\mu = 0)$, the Reynolds number is infinite. In other case, when there are no inertia effects, the Reynolds number is zero. However, the nature of flow pattern in an actual scenario depends strongly on Reynolds number and it falls in these two extremes either $\mathrm{Re} \gg 1$ or $\mathrm{Re} \ll 1$. The typical external flows with air/water are associated moderately sized objects with certain characteristics length $(0.01\mathrm{m} < l < 10\mathrm{m})$ and

free stream velocity $(0.1\text{m/s} < U < 100\,\text{m/s})$ that results Reynolds number in the range $10 < \text{Re} < 10^9$. So, as a rule of thumb, the flows with $\text{Re} \gg 1$, are dominated by viscous effects and inertia effects become predominant when $\text{Re} > 100$. Hence, the most familiar external flows are dominated by inertia. So, the objective of this section is to quantify the behavior of viscous, incompressible fluids in external flow.

Let us discuss few important features in an external flow past an airfoil (Fig. 5.7.1) where the flow is dominated by inertial effects. Some of the important features are highlighted below;

- The free stream flow divides at the stagnation point.
- The fluid at the body takes the velocity of the body (no-slip condition).
- A boundary layer is formed at the upper and lower surface of the airfoil.
- The flow in the boundary layer is initially laminar and the transition to turbulence takes place at downstream of the stagnation point, depending on the free stream conditions.
- The turbulent boundary layer grows more rapidly than the laminar layer, thus thickening the boundary layer on the body surface. So, the flow experiences a thicker body compared to original one.
- In the region of increasing pressure (adverse pressure gradient), the flow separation may occur. The fluid inside the boundary layer forms a viscous wake behind the separated points.

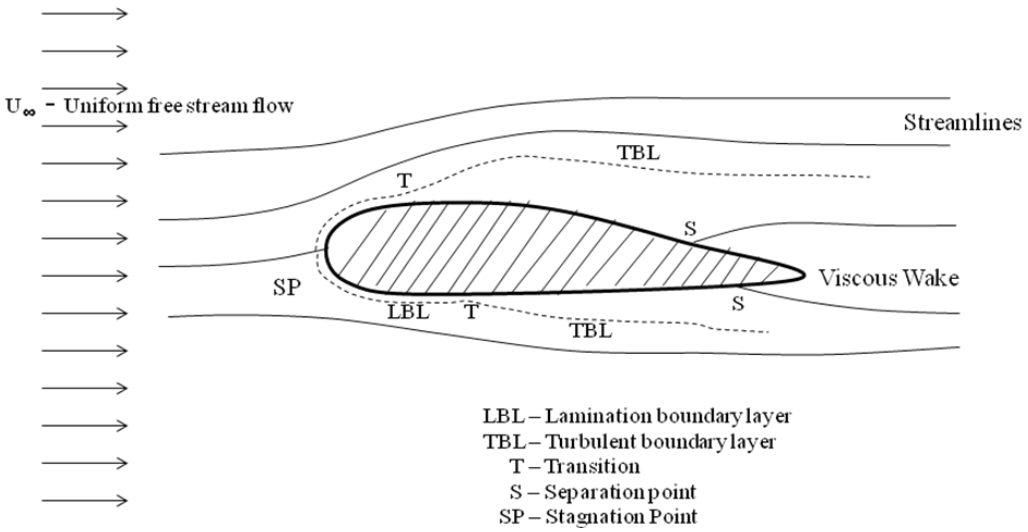

Fig. 5.7.1: Important features in an external flow.

Boundary Layer Characteristics

The concept of boundary layer was first introduced by a German scientist, Ludwig Prandtl, in the year 1904. Although, the complete descriptions of motion of a viscous fluid were known through Navier-Stokes equations, the mathematical difficulties in solving these equations prohibited the theoretical analysis of viscous flow. Prandtl suggested that the viscous flows can be analyzed by dividing the flow into two regions; one close to the solid boundaries and other covering the rest of the flow. Boundary layer is the regions close to the solid boundary where the effects of viscosity are experienced by the flow. In the regions outside the boundary layer, the effect of viscosity is negligible and the fluid is treated as inviscid. So, the boundary layer is a buffer region between the wall below and the inviscid free-stream above. This approach allows the complete solution of viscous fluid flows which would have been impossible through Navier-Stokes equation. The qualitative picture of the boundary-layer growth over a flat plate is shown in Fig. 5.7.2.

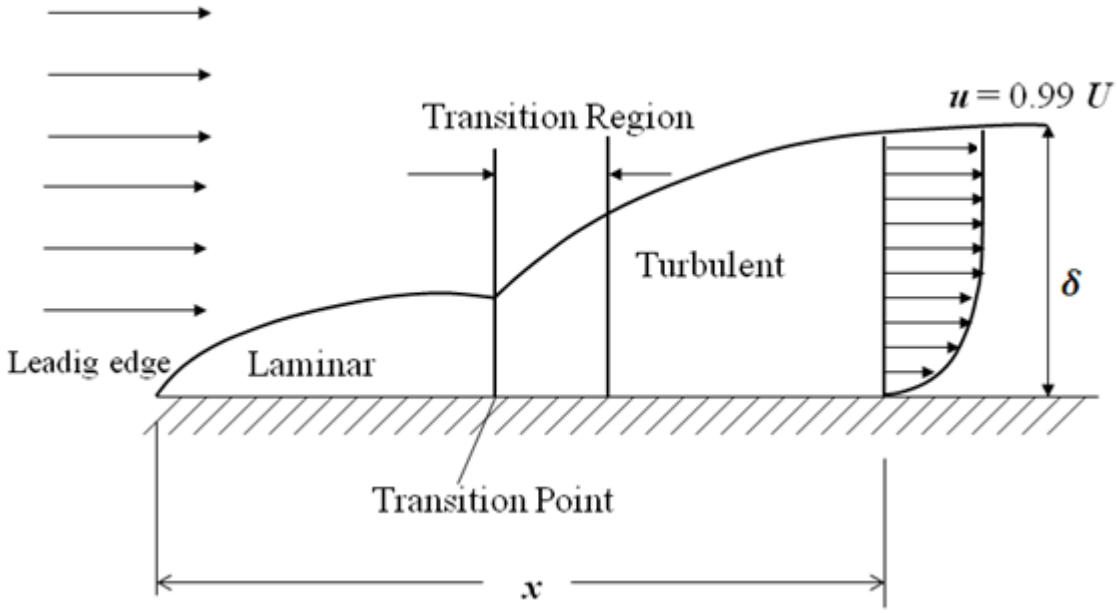

Fig. 5.7.2: Representation of boundary layer on a flat plate.

A laminar boundary layer is initiated at the leading edge of the plate for a short distance and extends to downstream. The transition occurs over a region, after certain length in the downstream followed by fully turbulent boundary layers. For common calculation purposes, the transition is usually considered to occur at a distance where the Reynolds number is about 500,000. With air at standard conditions, moving at a velocity of 30m/s, the transition is expected to occur at a distance of about 250mm. A typical boundary layer flow is characterized by certain parameters as given below;

Boundary layer thickness (δ): It is known that no-slip conditions have to be satisfied at the solid surface: the fluid must attain the zero velocity at the wall. Subsequently, above the wall, the effect of viscosity tends to reduce and the fluid within this layer will try to approach the free stream velocity. Thus, there is a velocity gradient that develops within the fluid layers inside the small regions near to solid surface. The *boundary layer thickness* is defined as the distance from the surface to a point where the velocity is reaches 99% of the free stream velocity. Thus, the velocity profile merges smoothly and asymptotically into the free stream as shown in Fig. 5.7.3(a).

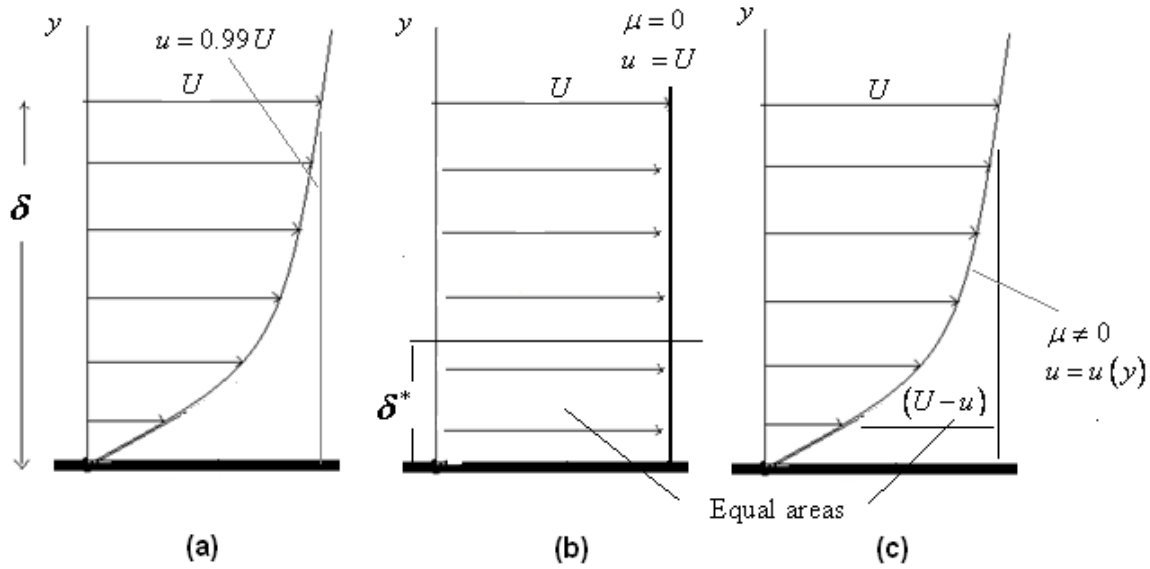

Fig. 5.7.3: (a) Boundary layer thickness; (b) Free stream flow (no viscosity); (c) Concepts of displacement thickness.

Displacement thickness $\left(\delta^*\right)$: The effect of viscosity in the boundary layer is to retard the flow. So, the mass flow rate adjacent to the solid surface is less than the mass flow rate that would pass through the same region in the absence of boundary layer. In the absence of viscous forces, the velocity in the vicinity of sold surface would be U as shown in Fig. 5.7.3(b). The decrease in the mass flow rate due to the influence of viscous forces is $\int_0^\infty \rho\left(U-u\right)b\,dy$, where b is the width of the surface in the direction perpendicular to the flow. So, the *displacement thickness* is the distance by which the solid boundary would displace in a frictionless flow (Fig. 5.7.3-b) to give rise to same mass flow rate deficit as exists in the boundary layer (Fig. 5.7.3-c). The mass flow rate deficiency by displacing the solid boundary by δ^* will be $\rho U\,\delta^* b$. In an incompressible flow, equating these two terms, the expression for δ^* is obtained.

$$\begin{aligned}&\rho U\,\delta^* b=\int_0^\infty \rho\left(U-u\right)b\,dy\\&\Rightarrow \delta^*=\int_0^\infty\left(1-\frac{u}{U}\right)dy\approx\int_0^\delta\left(1-\frac{u}{U}\right)dy\end{aligned}\tag{5.7.1}$$

Momentum thickness $\left(\theta^*\right)$: The flow retardation in the boundary layer also results the reduction in momentum flux as compared to the inviscid flow. The momentum thickness is defined as the thickness of a layer of fluid with velocity U, for which the momentum flux is equal to the deficit of momentum flux through the boundary layer. So, the expression for θ^* in an incompressible flow can be written as follow;

$$\begin{aligned}&\rho U^2\,\theta^*=\int_0^\infty \rho u\left(U-u\right)\,dy\\&\Rightarrow \theta^*=\int_0^\infty\frac{u}{U}\left(1-\frac{u}{U}\right)dy\approx\int_0^\delta\frac{u}{U}\left(1-\frac{u}{U}\right)dy\end{aligned}\tag{5.7.2}$$

The displacement/momentum thickness has the following physical implications;

- The displacement thickness represents the amount of distance that thickness of the body must be increased so that the fictitious uniform inviscid flow has the same mass flow rate properties as the actual flow.
- It indicates the outward displacement of the streamlines caused by the viscous effects on the plate.

- The flow conditions in the boundary layer can be simulated by adding the displacement thickness to the actual wall thickness and thus treating the flow over a thickened body as in the case of inviscid flow.
- Both δ^* and θ^* are the integral thicknesses and the integrant vanishes in the free stream. So, it is relatively easier to evaluate δ^* and θ^* as compared to δ.

The boundary layer concept is based on the fact that the boundary layer is thin. For a flat plate, the flow at any location *x* along the plate, the boundary layer relations $\left(\delta \square\ x;\ \delta^* \square\ x \text{ and } \theta^* \square\ x\right)$ are true except for the leading edge. The velocity profile merges into the local free stream velocity asymptotically. The pressure variation across the boundary layer is negligible i.e. same free stream pressure is impressed on the boundary layer. Considering these aspects, an approximate analysis can be made with the following assumptions within the boundary layer.

$$\begin{aligned} &\text{At } y = \delta \Rightarrow u \to U \\ &\text{At } y = \delta \Rightarrow \left(\partial u/\partial y\right) \to 0 \\ &\text{Within the boundary layer, } v \square\ U \end{aligned} \qquad (5.7.3)$$

Module 5 : Lecture 8
VISCOUS INCOMPRESSIBLE FLOW
(External Flow – Part II)

Boundary Layer Equations

There are two general flow situations in which the viscous terms in the Navier-Stokes equations can be neglected. The first one refers to high Reynolds number flow region where the net viscous forces are negligible compared to inertial and/or pressure forces, thus known as *inviscid flow region*. In the other cases, there is no vorticity (irrotational flow) in the flow field and they are described through potential flow theory. In either case, the removal of viscous terms in the Navier-Stokes equation yields Euler equation. When there is a viscous flow over a stationary solid wall, then it must attain zero velocity at the wall leading to non-zero viscous stress. The Euler's equation has the inability to specify no-slip condition at the wall that leads to un-realistic physical situations. The gap between these two equations is overcome through *boundary layer approximation developed by Ludwig Prandtl* (1875-1953). The idea is to divide the flow into two regions: outer inviscid/irrotational flow region and *boundary laye*r region. It is a very thin inner region near to the solid wall where the vorticity/irrotationality cannot be ignored. The flow field solution of the inner region is obtained through boundary layer equations and it has certain assumptions as given below;

- The thickness of the boundary layer (δ) is very small. For a given fluid and plate, if the Reynolds number is high, then at any given location (x) on the plate, the boundary layer becomes thinner as shown in Fig. 5.8.1(a).
- Within the boundary layer (Fig. 5.8.1-b), the component of velocity normal to the wall is very small as compared to tangential velocity $(v \ll u)$.
- There is no change in pressure across the boundary layer i.e. pressure varies only in the *x*-direction.

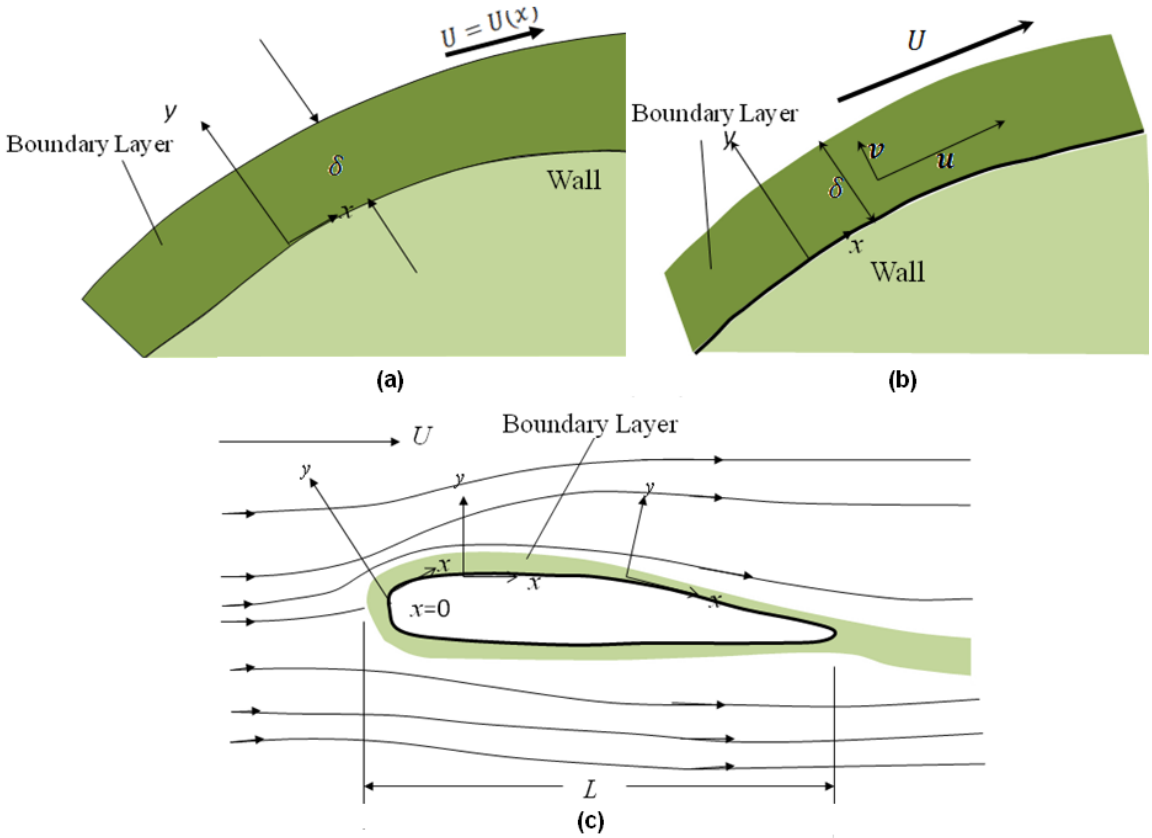

Fig. 5.8.1: Boundary layer representation: (a) Thickness of boundary layer; (b) Velocity components within the boundary layer; (c) Coordinate system used for analysis within the boundary layer.

After having some physical insight into the boundary layer flow, let us generate the boundary layer equations for a steady, laminar and two-dimensional flow in *x*-*y* plane as shown in Fig. 5.8.1(c). This methodology can be extended to axi-symmetric/three-dimensional boundary layer with any coordinate system. Within the boundary-layer as shown in Fig. 5.8.1(c), a coordinate system is adopted in which *x* is parallel to the wall everywhere and *y* is the direction normal to the wall. The location $x = 0$ refers to stagnation point on the body where the free stream flow comes to rest. Now, take certain length scale (L) for distances in the stream-wise direction (x) so that the derivatives of velocity and pressure can be obtained. Within the boundary layer, the choice of this length scale (L) is too large compared to the boundary layer thickness (δ). So the scale L is not a proper choice for *y*-direction. Moreover, it is difficult to obtain the derivatives with respect to *y*. So, it is more appropriate to use a length scale of δ for the direction normal to the stream-wise direction. The characteristics velocity $U = U(x)$ is the velocity parallel to the wall at a location just above the

boundary layer and p_∞ is the free stream pressure. Now, let us perform *order of magnitude* analysis within the boundary layer;

$$u \sim U; \quad (p - p_\infty) \sim \rho U^2; \quad \frac{\partial}{\partial x} \sim \frac{1}{L}; \quad \frac{\partial}{\partial y} \sim \frac{1}{\delta} \tag{5.8.1}$$

Now, apply Eq. (5.8.1) in continuity equation to obtain order of magnitude in *y*-component of velocity.

$$\frac{\partial u}{\partial x} + \frac{\partial v}{\partial y} = 0 \quad \Rightarrow \frac{U}{L} \sim \frac{v}{\delta} \quad \Rightarrow v \sim \frac{U\delta}{L} \tag{5.8.2}$$

Consider the momentum equation in the *x* and *y* directions;

$$\begin{aligned} x-\text{momentum}: u\frac{\partial u}{\partial x} + v\frac{\partial u}{\partial y} &= -\frac{1}{\rho}\left(\frac{dP}{dx}\right) + \nu\left(\frac{\partial^2 u}{\partial x^2} + \frac{\partial^2 u}{\partial y^2}\right) \\ y-\text{momentum}: u\frac{\partial v}{\partial x} + v\frac{\partial v}{\partial y} &= -\frac{1}{\rho}\left(\frac{\partial P}{\partial y}\right) + \nu\left(\frac{\partial^2 v}{\partial x^2} + \frac{\partial^2 v}{\partial y^2}\right) \end{aligned} \tag{5.8.3}$$

Here, $\nu\left(=\frac{\mu}{\rho}\right)$ is the kinematic viscosity. Let us define non-dimensional variables within the boundary layer as follows:

$$x^* = \frac{x}{L}; \; y^* = \frac{y}{\delta}; \; u^* = \frac{u}{U}; \; v^* = \frac{vL}{U\delta}; \; p^* = \frac{p - p_\infty}{\rho U^2} \tag{5.8.4}$$

First, apply Eq. (5.8.4) in *y*-momentum equation, multiply each term by $L^2/\left(U^2\delta\right)$ and after simplification, one can obtain the non-dimensional form of *y* – momentum equation.

$$\begin{aligned} &u^*\frac{\partial v^*}{\partial x^*} + v^*\frac{\partial v^*}{\partial y^*} = -\left(\frac{L}{\delta}\right)^2\frac{\partial p^*}{\partial y^*} + \left(\frac{\nu}{UL}\right)\frac{\partial^2 v^*}{\partial x^{*2}} + \left(\frac{\nu}{UL}\right)\left(\frac{L}{\delta}\right)^2\frac{\partial^2 v^*}{\partial y^{*2}} \\ &\text{or, } u^*\frac{\partial v^*}{\partial x^*} + v^*\frac{\partial v^*}{\partial y^*} + \left(\frac{L}{\delta}\right)^2\frac{\partial p^*}{\partial y^*} = \left(\frac{1}{\text{Re}}\right)\frac{\partial^2 v^*}{\partial x^{*2}} + \left(\frac{1}{\text{Re}}\right)\left(\frac{L}{\delta}\right)^2\frac{\partial^2 v^*}{\partial y^{*2}} \end{aligned} \tag{5.8.5}$$

For boundary layer flows, the Reynolds number is considered as very high which means the second and third terms in the RHS of Eq. (5.8.5) can be neglected. Further, the pressure gradient term is much higher than the convective terms in the LHS of Eq. (5.8.5), because $L \gg \delta$. So, the non-dimensional *y*-momentum equation reduces to,

$$\frac{\partial p^*}{\partial y^*} \cong 0 \quad \Rightarrow \frac{\partial p}{\partial y} = 0 \tag{5.8.6}$$

It means the pressure across the boundary layer (y-direction) is nearly constant i.e. negligible change in pressure in the direction normal to the wall (Fig. 5.8.2-a). This leads to the fact that the streamlines in the thin boundary layer region have negligible curvature when observed at the scale of δ. However, the pressure may vary along the wall (x-direction). Thus, y-momentum equation analysis suggests the fact that pressure across the boundary layer is same as that of inviscid outer flow region. Hence, one can apply Bernoulli equation to the outer flow region and obtain the pressure variation along x-direction where both p and U are functions of x only (Fig. 5.8.2-b).

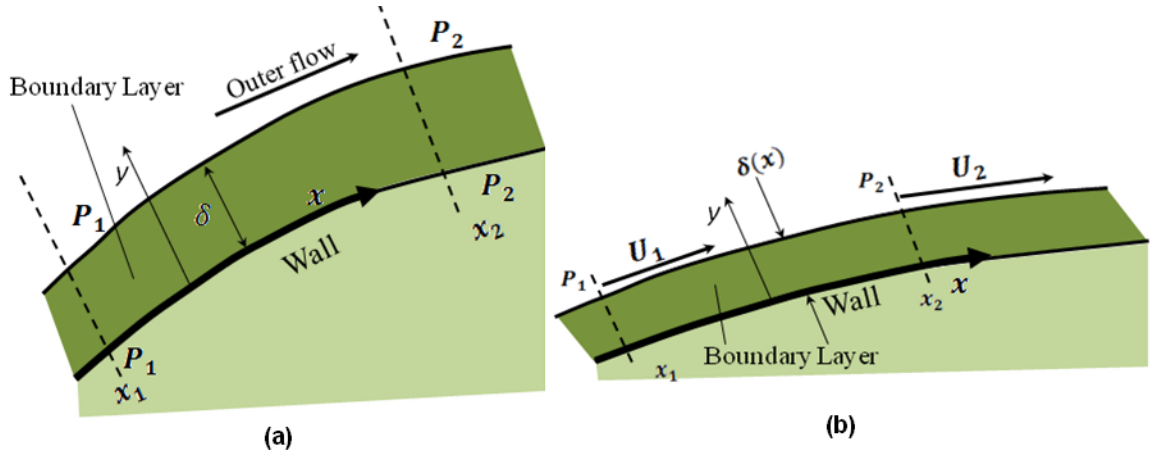

Fig. 5.8.2: Variation of pressure within the boundary layer: (a) Normal to the wall; (b) Along the wall.

$$\frac{p}{\rho}+\frac{1}{2}U^2=\text{constant} \quad \Rightarrow \frac{1}{\rho}\frac{dp}{dx}=-U\frac{dU}{dx} \tag{5.8.7}$$

Next, apply Eq. (5.8.4) in x – momentum equation, multiply each term by $\left(L/U^2\right)$ and after simplification, one can obtain the non-dimensional form of x– momentum equation.

$$\begin{aligned} &u^*\frac{\partial u^*}{\partial x^*}+v^*\frac{\partial u^*}{\partial y^*}=-\frac{dp^*}{dx^*}+\left(\frac{\nu}{UL}\right)\frac{\partial^2 u^*}{\partial x^{*2}}+\left(\frac{\nu}{UL}\right)\left(\frac{L}{\delta}\right)^2\frac{\partial^2 u^*}{\partial y^{*2}} \\ &\text{or, } u^*\frac{\partial u^*}{\partial x^*}+v^*\frac{\partial u^*}{\partial y^*}=\frac{\partial p^*}{\partial x^*}+\left(\frac{1}{\text{Re}}\right)\frac{\partial^2 u^*}{\partial x^{*2}}+\left(\frac{1}{\text{Re}}\right)\left(\frac{L}{\delta}\right)^2\frac{\partial^2 u^*}{\partial y^{*2}} \end{aligned} \tag{5.8.8}$$

It may be observed that all the terms in the LHS and first term in the RHS of Eq. (5.8.8) are of the order unity. The second term of RHS can be neglected because the Reynolds number is considered as very high. The last term of Eq. (5.8.8) is equivalent to inertia term and thus it has to be the order of one.

$$\left(\frac{\nu}{UL}\right)\left(\frac{L}{\delta}\right)^2 \sim 1 \quad \Rightarrow \frac{U^2}{L} \sim \nu\frac{U}{\delta^2} \Rightarrow \frac{\delta}{L} \sim \frac{1}{\sqrt{\mathrm{Re}_L}} \tag{5.8.9}$$

Eq. (5.8.9) clearly shows that the convective flux terms are of same order of magnitudes of viscous diffusive terms. Now, neglecting the necessary terms and with suitable approximations, the equations for a steady, incompressible and laminar boundary flow can be obtained from Eqs (5.8.2 & 5.8.3). They are written in terms of physical variables in *x*-*y* plane as follows;

$$\begin{aligned}
&\text{Continuity}: \quad \frac{\partial u}{\partial x}+\frac{\partial v}{\partial y}=0 \\
&x-\text{momentum}: u\frac{\partial u}{\partial x}+v\frac{\partial u}{\partial y}=U\frac{dU}{dx}+\nu\frac{\partial^2 u}{\partial y^2} \\
&y-\text{momentum}: \frac{\partial p}{\partial y}=0
\end{aligned} \tag{5.8.10}$$

Solution Procedure for Boundary Layer

Mathematically, a full Navier-Stokes equation is elliptic in space which means that the boundary conditions are required in the entire flow domain and the information is passed in all directions, both upstream and downstream. However, with necessary boundary layer approximations, the *x* – momentum equation is parabolic in nature which means the boundary conditions are required only three sides of flow domain (Fig. 5.8.3-a). So, the stepwise procedure is outlined here.

- Solve the outer flow with inviscid/irrotational assumptions using Euler's equation and obtain the velocity field as $U(x)$. Since the boundary layer is very thin, it does not affect the outer flow solution.
- With some known starting profile $\left(x = x_s \Rightarrow u = u_s(y)\right)$, solve the Eq. (5.8.10) with no-slip conditions at the wall $\left(y = 0 \Rightarrow u = v = 0\right)$and known outer flow condition at the edge of the boundary layer $\left(y \to \infty \Rightarrow u = U(x)\right)$
- After solving Eq. (5.8.10), one can obtain all the boundary layer parameters such as displacement and momentum thickness.

Even though the boundary layer equations (Eq. 5.8.10) and the boundary conditions seem to be simple, but no analytical solution has been obtained so far. It was first solved numerically in the year 1908 by *Blasius*, for a simple flat plate. Nowadays, one can solve these equations with highly developed computer tools. It will be discussed in the subsequent section.

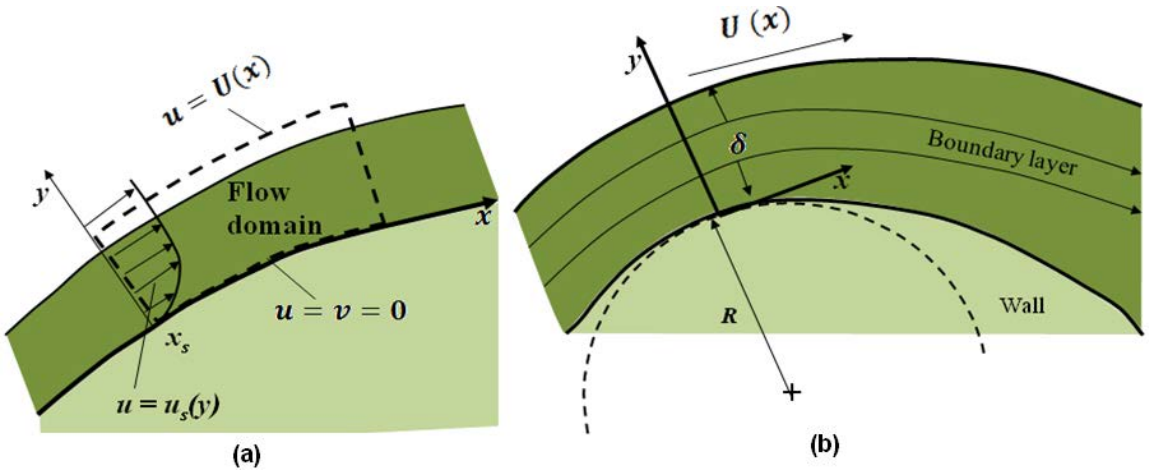

Fig. 5.8.3: Boundary layer calculations: (a) Initial condition and flow domain; (b) Effect of centrifugal force.

Limitations of Boundary Calculations

- The boundary layer approximation fails if the Reynolds number is not very large. Referring to Eq. (5.8.9), one can interpret $(\delta/L) \sim 0.001 \Rightarrow \mathrm{Re}_L \sim 10000$.
- The assumption of zero-pressure gradient does not hold good if the wall curvature is of similar magnitude as of δ because of centrifugal acceleration (Fig. 5.8.3-b).
- If the Reynolds number is too high $\mathrm{Re}_L \sim 10^5$, then the boundary layer does not remain laminar rather the flow becomes transitional or turbulent. Subsequently, if the flow separation occurs due to adverse pressure gradient, then the parabolic nature of boundary layer equations is lost due to flow reversal.

Module 5 : Lecture 9
VISCOUS INCOMPRESSIBLE FLOW
(External Flow – Part III)

Laminar Boundary Layer on a Flat Plate

Consider a uniform free stream of speed (U) that flows parallel to an infinitesimally thin semi-infinite flat plate as shown in Fig. 5.9.1(a). A coordinate system can be defined such that the flow begins at *leading edge* of the plate which is considered as the origin of the plate. Since the flow is symmetric about *x*-axis, only the upper half of the flow can be considered. The following assumptions may be made in the discussions;

- The nature of the flow is steady, incompressible and two-dimensional.
- The Reynolds number is high enough that the boundary layer approximation is reasonable.
- The boundary layer remains laminar over the entire flow domain.

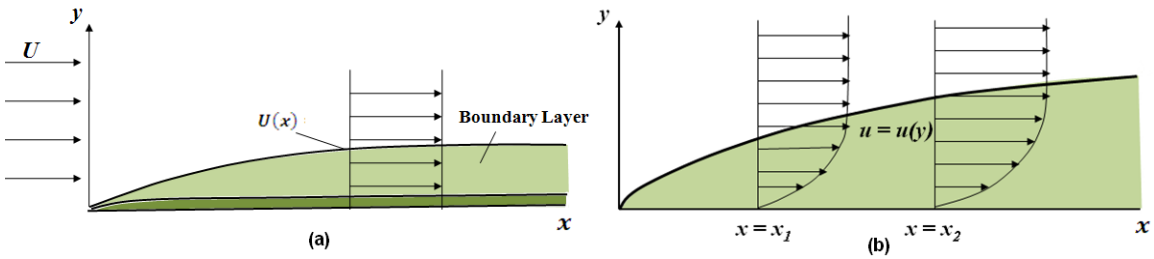

Fig. 5.9.1: Boundary layer on a flat plate: (a) Outer inviscid flow and thin boundary layer; (b) Similarity behavior of boundary layer at any x-location.

The outer flow is considered without the boundary layer and in this case, U is a constant so that $U\dfrac{dU}{dx}=0$. Referring to Fig. 5.9.1, the boundary layer equations and its boundary conditions can be written as follows;

$$\frac{\partial u}{\partial x}+\frac{\partial v}{\partial y}=0; \qquad u\frac{\partial u}{\partial x}+v\frac{\partial u}{\partial y}=\nu\frac{\partial^2 u}{\partial y^2}; \quad \frac{\partial p}{\partial y}=0 \tag{5.9.1}$$

Boundary conditions:

$$\begin{aligned} &u=0 \text{ at } y=0 \text{ and } u=U; \frac{du}{dy}=0 \text{ at } y\to\infty \\ &v=0 \text{ at } y=0 \text{ and } u=U \text{ for all } y \text{ at } x=0 \end{aligned} \tag{5.9.2}$$

No analytical solution is available till date for the above boundary layer equations. However, this equation was solved first by numerically in the year 1908 by *P.R.Heinrich Blasius* and commonly known as *Blasius solution for laminar boundary layer over a flat plate*. The key for the solution is the assumption of *similarity* which means there is no characteristics length scale in the geometry of the problem. Physically, it is the case for the same flow patterns for an infinitely long flat plate regardless of any close-up view (Fig. 5.9.1-b). So, mathematically a *similarity variable* (η) can be defined that combines the independent variables *x and y* into a non-dimensional independent variable. In accordance with the similarity law, the velocity profile is represented in the functional form;

$$\frac{u}{U} = F\left(x, y, \nu, U\right) = F\left(\eta\right) \quad \Rightarrow u = U\left\{F\left(\eta\right)\right\} \tag{5.9.3}$$

With the *order of magnitude* analysis, the thickness of the boundary layer is interpreted as $\delta \sqrt{\frac{\nu x}{U}}$. Based on this analogy, *Blasius* set the non-dimensional similarity variable in the following functional form;

$$\eta = y\sqrt{\frac{U}{\nu x}} \quad \Rightarrow \frac{d\eta}{dx} = -\frac{\eta}{2x} \text{ and } \frac{d\eta}{dy} = \sqrt{\frac{U}{\nu x}} \tag{5.9.4}$$

Now, let us introduce the stream function (ψ) for the two-dimensional flow.

$$u = \frac{\partial \psi}{\partial y} \text{ and } v = -\frac{\partial \psi}{\partial x} \tag{5.9.5}$$

The stream function can be obtained through integration of Eq. (5.9.5) and using the results of Eqs (5.9.3 & 5.9.4).

$$\psi = \int u\, dy = \int U\, F\left(\eta\right)\sqrt{\frac{\nu x}{U}} d\eta = \sqrt{U\nu x}\int F\left(\eta\right) d\eta = \sqrt{U\nu x}\ f\left(\eta\right) \tag{5.9.6}$$

Again, differentiate Eq. (5.9.6) with respect to *y* and use Eq. (5.9.4) to obtain the *x*-component of velocity profile within the boundary layer as function η (Fig. 5.9.2).

$$u = \frac{\partial \psi}{\partial y} = \sqrt{U\nu x}\left(\frac{\partial f}{\partial \eta}\right)\left(\frac{\partial \eta}{\partial y}\right) = U\ f'\left(\eta\right) \quad \Rightarrow \frac{u}{U} = f'\left(\eta\right) \tag{5.9.7}$$

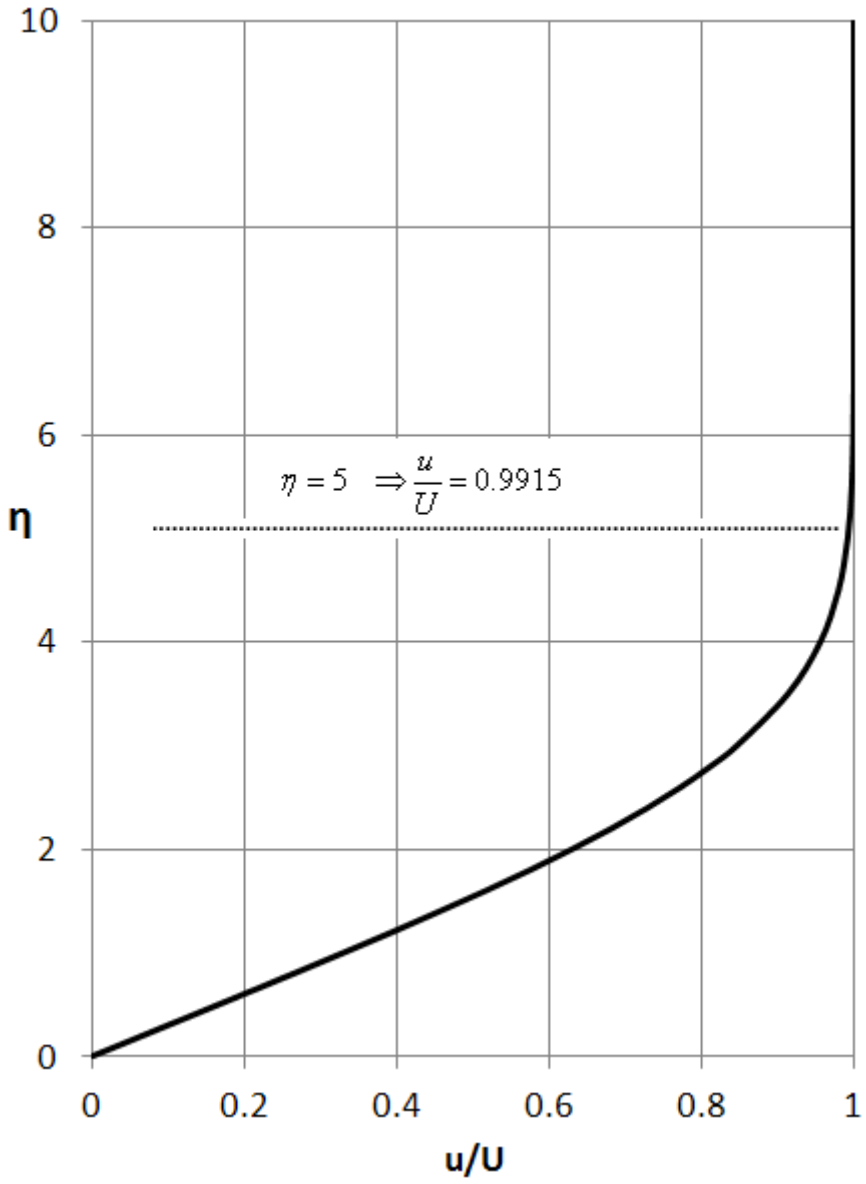

Fig. 5.9.2: Blasius profile for a laminar boundary layer over a flat plate.

The *y*-component of velocity profile can be obtained by differentiating stream function with respect to *x* and substituting the results from Eq. (5.9.4 & 5.9.6).

$$v = -\frac{\partial \psi}{\partial x} = -\frac{\partial}{\partial x}\left[\sqrt{U\nu x}\, f(\eta)\right] = -\left[\frac{1}{2}\sqrt{\frac{U\nu}{x}} f(\eta) + \sqrt{U\nu x}\left(\frac{\partial f}{\partial \eta}\right)\left(\frac{\partial \eta}{\partial x}\right)\right]$$
$$= -\left[\frac{1}{2}\sqrt{\frac{U\nu}{x}} f(\eta) - \frac{1}{2}\sqrt{\frac{U\nu}{x}}\eta f'(\eta)\right] = \frac{1}{2}\sqrt{\frac{U\nu}{x}}\left[\eta f'(\eta) - f(\eta)\right] \tag{5.9.8}$$

Now, let us calculate each term of Eq. (5.9.1) from the velocity components obtained from Eqs (5.9.7 & 5.9.8).

$$\frac{\partial u}{\partial x} = -\frac{U}{2x}\eta f''(\eta);\ \frac{\partial u}{\partial y} = U\, f''(\eta)\sqrt{\frac{U}{\nu x}};\ \frac{\partial^2 u}{\partial y^2} = \frac{U^2}{\nu x} f'''(\eta)$$
$$u = U\, f'(\eta);\ v = \frac{1}{2}\sqrt{\frac{U\nu}{x}}\left[\eta f'(\eta) - f(\eta)\right] \tag{5.9.9}$$

Substitute each term of Eq. (5.9.9) in Eq. (5.9.1) and after simplification, the boundary layer equation reduces to *Blasius* equation expressed in terms of similarity variable.

$$2f''' + f\ f'' = 0 \ \Rightarrow f''' + \frac{1}{2} f\ f'' = 0 \tag{5.9.10}$$

Table 5.9.1: Solution of *Blasius* laminar flat plate boundary layer in similarity variables

$\eta = y\sqrt{\frac{U}{\nu x}}$	$f(\eta)$	$f'(\eta) = \frac{u}{U}$	$f''(\eta)$
0	0	0	0.3321
1	0.1656	0.3298	0.3230
2	0.650	0.6298	0.2668
3	1.3968	0.8460	0.1614
4	2.3057	0.9555	0.0642
5	3.2833	0.9915	0.0159
6	4.2796	0.9990	0.0024
7	5.2792	0.9999	0.0002
8	6.2792	1.0	0
9	7.2792	1.0	0
10	8.2792	1.0	0

In certain cases, one can define $\eta = y\sqrt{\frac{U}{2\nu x}}$ and $\psi = \sqrt{2U\nu x}\, f(\eta)$ for which Eq. (5.9.10) takes the following form;

$$f''' + f\, f'' = 0 \tag{5.9.11}$$

The Blasius equation is a third-order non-linear ordinary differential equation for which the boundary conditions can be set using Eq. (5.9.2).

$$\begin{aligned} &y = 0;\ u = 0 && \Rightarrow \eta = 0,\ f' = 0 \\ &y = 0;\ v = 0 && \Rightarrow \eta = 0,\ f = f' = 0 \\ &y \to \infty;\ u = U && \Rightarrow \eta = \infty,\ f' = 1 \end{aligned} \tag{5.9.12}$$

The popular *Runge-Kutta numerical technique* can be applied for Eqs (5.9.11 & 5.9.12) to obtain the similarity solution in terms of η and some of the values are given in the Table 5.9.1.

Estimation of Boundary Layer Parameters

Boundary layer thickness (δ): It is defined as the distance away from the wall at which the velocity component parallel to the wall is 99% of the fluid speed outside the boundary layer. From Table 5.9.1, it is seen that $f'(\eta) = \frac{u}{U} = 0.99$ at $\eta = 5$. So, replacing $y = \delta$ in Eq. (5.9.4), one can obtain the following expression for boundary layer thickness;

$$\delta = \frac{5}{\sqrt{\frac{U}{\nu x}}} = \frac{5x}{\sqrt{\frac{Ux}{\nu}}} = \frac{5x}{\sqrt{\mathrm{Re}_x}} \quad \Rightarrow \frac{\delta}{x} = \frac{5}{\sqrt{\mathrm{Re}_x}} \text{ and } \delta \propto x^{\frac{1}{2}} \tag{5.9.13}$$

At this point, the transverse velocity can be calculated from Eq. (5.9.8).

For $\eta = 5$, $f(\eta) = 3.2833$ and $f'(\eta) = 0.9915$

$$\frac{v}{U} = \frac{1}{2\sqrt{\frac{Ux}{\nu}}}\left[\eta f'(\eta) - f(\eta)\right] = \frac{1}{2\sqrt{\mathrm{Re}_x}}\left[\eta f'(\eta) - f(\eta)\right] \quad \Rightarrow \frac{v}{U} = \frac{0.84}{\sqrt{\mathrm{Re}_x}} \tag{5.9.14}$$

Displacement thickness $\left(\delta^*\right)$: It is the distance that a streamline just outside of the boundary layer is deflected away from the wall due to the effect of the boundary layer. Mathematically, it can be represented in terms of transformed variable using Eq. (5.9.4).

$$\delta^* = \int_0^{\delta}\left(1-\frac{u}{U}\right)dy = \sqrt{\frac{\nu x}{U}}\int_0^{\eta}\left[1-f'(\eta)\right]d\eta = = \sqrt{\frac{\nu x}{U}}\ \left[\eta - f(\eta)\right] \qquad (5.9.15)$$

It may be seen from the Table 5.9.1 that for all values of $\eta > 5$, the functional value of Eq. (5.9.15) is always a constant quantity i.e. $\left[\eta - f(\eta)\right] = 1.72$. So, Eq. (5.9.15) can be simplified in terms of Reynolds number;

$$\frac{\delta^*}{x} = \frac{1.72}{\sqrt{\mathrm{Re}_x}} \qquad (5.9.16)$$

Momentum thickness $\left(\theta^*\right)$: It is defined as the loss of momentum flux per unit width divided by ρU^2 due to the presence of the growing boundary layer. Mathematically, it can be represented in terms of transformed variable using Eq. (5.9.4).

$$\theta^* = \int_0^{\delta}\frac{u}{U}\left(1-\frac{u}{U}\right)dy = \sqrt{\frac{\nu x}{U}}\int_0^{\eta} f'(\eta)\left[1-f'(\eta)\right]d\eta \qquad (5.9.17)$$

This integration is carried out numerically from $\eta = 0$ to any arbitrary point $\eta > 5$ and the results give rise to the following relation;

$$\frac{\theta^*}{x} = \frac{0.664}{\sqrt{\mathrm{Re}_x}} \qquad (5.9.18)$$

Comparing the Eqs (5.9.13, 5.9.16 & 5.9.18), it is seen that the all are inversely proportional to the square root of Reynolds number except the difference in magnitude. The value of δ^* is about 34% of δ while θ^* turns out to be approximately 13% of δ at any *x*-location (Fig. 5.9.3).

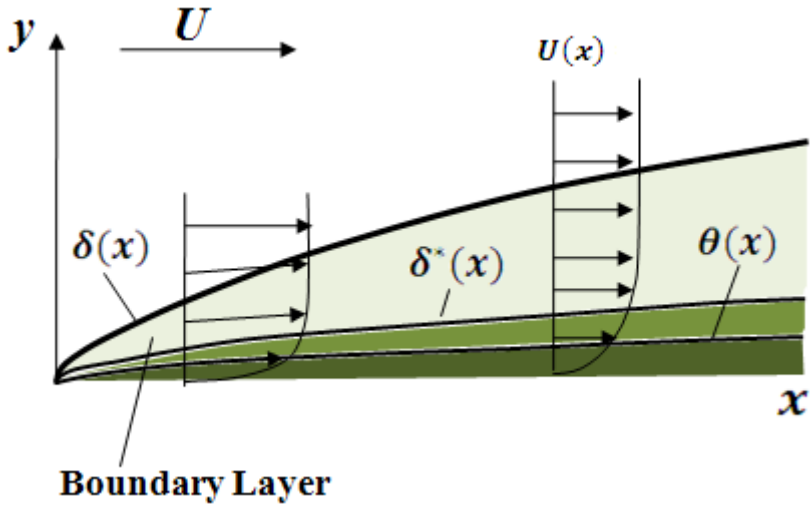

Fig. 5.9.3: Boundary layer thickness, displacement thickness and momentum thickness for a flat plate.

In order to correlate the data for variety of boundary layers under different conditions, a *dimensionless profile shape factor* is often defined as the ratio of displacement thickness to momentum thickness. For a flat plate laminar boundary layer,

$$H = \frac{\delta^*}{\theta^*} = 2.59 \tag{5.9.19}$$

Skin friction coefficient $\left(c_f\right)$: Analogous to friction factor in a duct/pipe flows, a non-dimensional parameter is defined for boundary layer flow as the *skin-friction coefficient* (Fig. 5.9.4). It relates the shear stress at the wall $\left(\tau_w\right)$ to the free stream dynamic pressure.

$$\begin{aligned} c_f &= \frac{\tau_w}{(1/2)\rho U^2} = \frac{\mu\left(\partial u/\partial y\right)_{y=0}}{(1/2)\rho U^2} = \frac{\mu\left[U\, f''(\eta)\left(\partial\eta/\partial y\right)\right]_{y=0}}{(1/2)\rho U^2} \\ &= \frac{\mu U\sqrt{U/\nu x}}{(1/2)\rho U^2} f''(0) = \frac{0.664}{\sqrt{\mathrm{Re}_x}} \end{aligned} \tag{5.9.20}$$

From Eqs (5.9.18 & 5.9.20), it is observed that the non-dimensional momentum thickness is identical to the skin friction coefficient. Further, the wall shear stress can be estimated from Eq. 5.9.20.

$$\tau_w = \frac{0.664}{2}\rho U^2\sqrt{\frac{\mu}{\rho U x}} = 0.332 U^{\frac{3}{2}}\sqrt{\frac{\rho\mu}{x}} \qquad (5.9.21)$$

It may be noted here that shear stress decreases with increase in the value of x because of the increase in the boundary layer thickness and decrease in velocity gradient at the wall along the direction of x. Also, τ_w varies directly with $U^{\frac{3}{2}}$ not as U which is the case for a fully-developed laminar pipe flow.

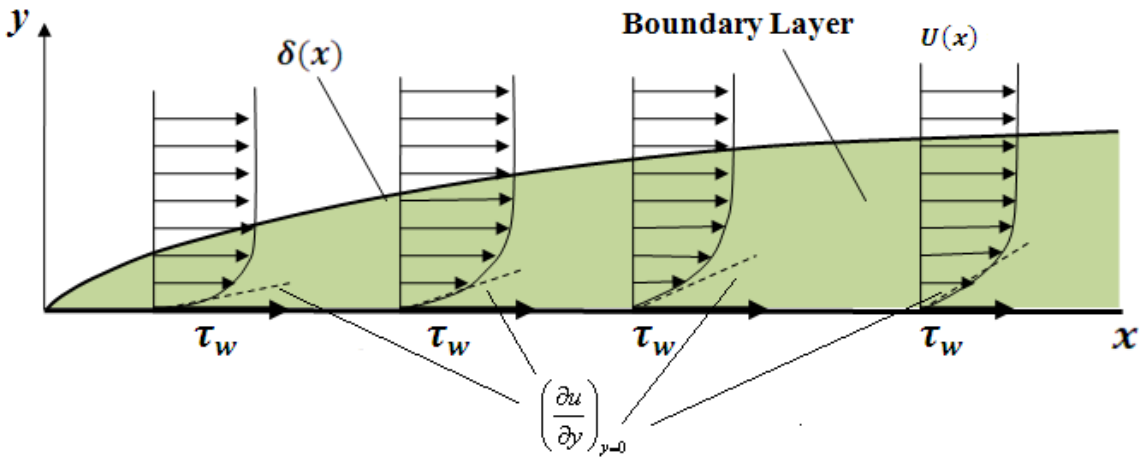

Fig. 5.9.4: Decay of wall shear stress due to decrease in slope at the wall.

Drag coefficient (c_d): The effect of skin friction/wall shear stress is to retard the free stream flow. It is quantified by skin friction coefficient at a particular *x*-location on the flat plate and is expressed by Eq. (5.9.20). When this parameter is integrated over the entire length of the plate, then total drag coefficient is obtained (Fig. 5.9.5). In terms of free stream parameter and wall shear stress, c_d is quantified as follows;

$$c_d = \frac{D}{(1/2)\rho U^2 A} = \frac{1}{L}\int_0^L c_f\, dx = \frac{0.664}{L}\sqrt{U/\nu L}\int_0^L x^{-1/2}\, dx = \frac{1.328}{\sqrt{\mathrm{Re}_L}} \tag{5.9.22}$$

Comparing Eqs (5.9.18 & 5.9.22), it is seen that skin friction drag coefficient for a flat plate is directly proportional to the values of θ^* evaluated at the trailing edge of the plate.

$$\left[\theta^*\right]_{x=L} = \frac{0.664\,L}{\sqrt{\mathrm{Re}_L}};\ c_d = \frac{1.328}{\sqrt{\mathrm{Re}_L}} = \frac{2\left[\theta^*\right]_{x=L}}{L} \tag{5.9.23}$$

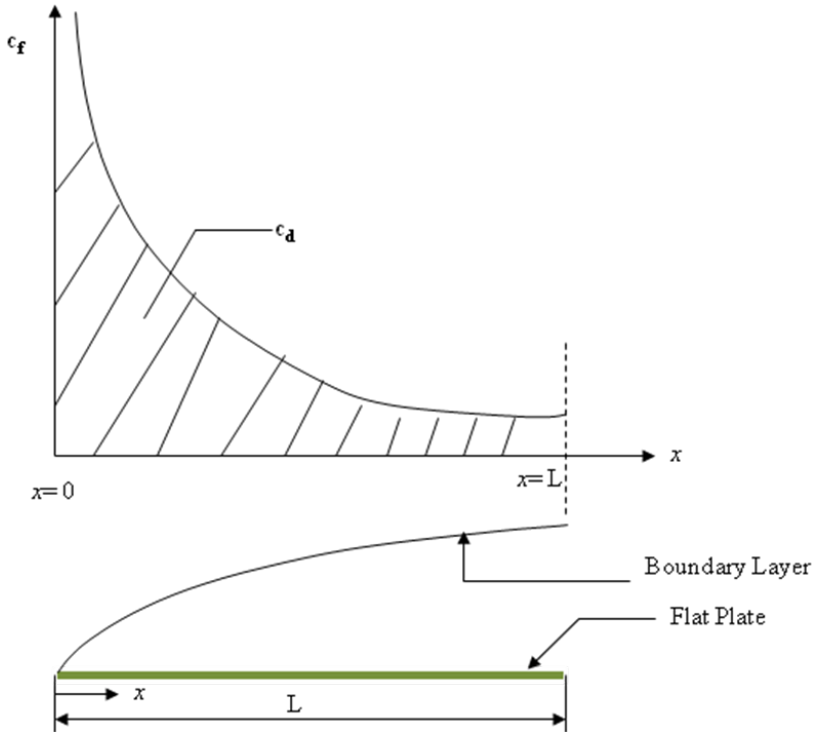

Fig. 5.9.5: Variation of skin friction coefficient along the length of a flat plate.

Module 5 : Lecture 10
VISCOUS INCOMPRESSIBLE FLOW
(External Flow – Part IV)

Momentum Integral Boundary Layer Relation for a Flat Plate

One of the important aspects of boundary layer theory is the determination of drag caused by the shear force on the body. With respect to flat plate, the drag coefficient is estimated through numerical solution of *Blasius equation* which is a third-order non-linear ordinary differential equation. In order to get rid of the differential equation, there is an alternative method by which the exact prediction of drag coefficient is possible. The *momentum integral method* is one of the alternative techniques by which boundary layer parameters can be predicted through control volume analysis.

Consider a uniform flow past a flat plate and the growth of boundary layer as shown in Fig. 5.10.1. A fixed control volume is chosen for which the uniform flow enters at the leading edge at the section '1'. At the exit of the control volume (section '1'), the velocity varies from zero (at the wall) to the free stream velocity (U) at the edge of the boundary layer. It is assumed that the pressure is constant throughout the flow field. The width and height of the control volume are taken as b and h, respectively.

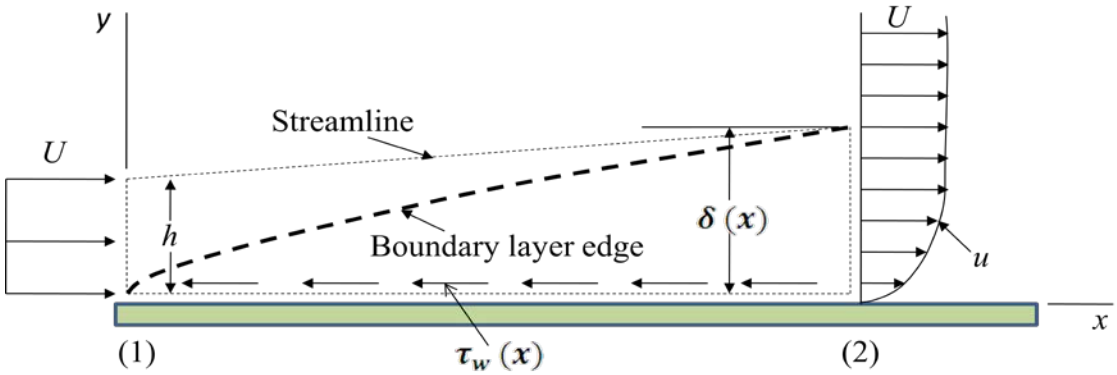

Fig. 5.10.1: Control volume analysis for the flat pate.

The drag force (D) on the plate can be obtained when the *x*-momentum equation is applied to the steady flow of fluid within this control volume. It is same as the integration of wall shear stress (τ_w) along the length of the plate (Fig. 5.10.1).

$$\sum F_x = -D = -\int \tau_w dA = -l\int \tau_w dx \quad \text{and}$$
$$\sum F_x = \rho\int_1 U\left(-U\right)dA + \rho\int_2 u^2\, dA \tag{5.10.1}$$

This equation leads to the expression for drag force as given below;

$$D = \rho U^2 bh - \rho l\int_0^\delta u^2 dA \tag{5.10.2}$$

Now, write the mass conservation equation, for the sections '1' and '2'.

$$Uh = \int_0^\delta u\, dA \quad \Rightarrow \rho U^2 bh = \rho b\int_0^\delta U\, u\, dA \tag{5.10.3}$$

The expression for drag force can be obtained by combining Eqs (5.10.2 & 5.10.3).

$$D = \rho b\int_0^\delta u\left(U-u\right)dA \tag{5.10.4}$$

Now, recall the expression for momentum thickness;

$$\theta^* = \int_0^\delta \frac{u}{U}\left(1-\frac{u}{U}\right)dy \quad \Rightarrow U^2\theta^* = \int_0^\delta u\left(U-u\right)dA \tag{5.10.5}$$

So, Eq. (5.10.4) can be rewritten as,

$$D = \rho b U^2\theta^* \quad \Rightarrow \frac{dD}{dx} = \rho b U^2\frac{d\,\theta^*}{dx} \tag{5.10.6}$$

It follows from Eqs (5.10.1) that $\frac{dD}{dx} = b\,\tau_w$ so that the wall-shear stress can be obtained through Eq. (5.10.6).

$$\tau_w = \rho U^2\frac{d\,\theta^*}{dx} \tag{5.10.7}$$

The usefulness of Eq. (5.10.7) lies in the ability to obtain wall shear stress from the velocity layer profile. It is known as the *momentum-integral relation*. Moreover, this equation is valid for laminar as well as turbulent flows.

Solution of Momentum Integral Relation

With the knowledge of a velocity profile within the boundary layer, the momentum integral equation can be used to obtain all the boundary layer parameters. In general, it is appropriate to assume certain velocity from the experimental data. Thus, the accuracy of the results depends on how closely the assumed profile approximates to the actual profile. Let us consider a general velocity profile in a boundary layer;

$$\frac{u}{U} = g(Y) \text{ for } 0 \le Y \le 1 \quad \text{and} \quad \frac{u}{U} = 1 \text{ for } Y > 1 \tag{5.10.8}$$

Here, the dimensionless parameter $Y = y/\delta$ varies from 0 to 1 across the boundary layer and one can assume the dimensionless function of any shape. Let is impose the boundary conditions and write the functions;

$$\begin{aligned} &y = 0 \;\Rightarrow\; g(Y) = 0,\; u = 0 \\ &y = \delta \;\Rightarrow\; g(Y) = 1,\; u = U,\; (dg/dY) = 0 \end{aligned} \tag{5.10.9}$$

For a given function $g(Y)$, one can calculate the drag force on the plate from Eq. (5.10.4).

$$\begin{aligned} &D = \rho b \int_0^{\delta} u(U-u)\,dA = \rho b U^2 \delta \int_0^1 g(Y)\left[1 - g(Y)\right] dY = \rho b U^2 \delta C_1 \\ &\text{or, } \frac{dD}{dx} = \rho b U^2 C_1 \left(\frac{d\delta}{dx}\right) = b\,\tau_w \end{aligned} \tag{5.10.10}$$

The wall shear stress can also be obtained in the following form;

$$\tau_w = \mu \left(\frac{\partial u}{\partial y}\right)_{y=0} = \left(\frac{\mu U}{\delta}\right)\left(\frac{dg}{dY}\right)_{Y=0} = \left(\frac{\mu U}{\delta}\right) C_2 \tag{5.10.11}$$

Here, $C_1 = \int_0^1 g(Y)\left[1 - g(Y)\right] dY$ is a dimensional constant and is evaluated with assumed velocity profile and $C_2 = \left(\frac{dg}{dY}\right)_{Y=0}$. Combining the Eqs (5.10.10 & 5.10.11) and integrating the resulting expression, one can obtain the following expression;

$$\delta\, d\delta = \left(\frac{\mu}{\rho U}\right)\left(\frac{C_2}{C_1}\right) dx \quad \Rightarrow \frac{\delta}{x} = \frac{\sqrt{2C_2/C_1}}{\sqrt{\mathrm{Re}_x}} \tag{5.10.12}$$

Substituting Eq. (5.10.12) back into Eq. 5.10.11, the expression of τ_w is obtained;

$$\tau_w = \sqrt{\frac{C_1 C_2}{2}}\, U^{\frac{3}{2}} \sqrt{\frac{\rho\mu}{x}} \tag{5.10.13}$$

The dimensionless local skin-friction coefficient is obtained as,

$$c_f = \frac{\tau_w}{(1/2)\rho U^2} = \frac{\sqrt{2C_1C_2}}{\sqrt{\mathrm{Re}_x}} \tag{5.10.14}$$

For a flat plate, of certain length (l) and width (b), the net friction drag is often expressed in terms of friction drag coefficient (C_{Df}).

$$C_{Df} = \frac{D}{(1/2)\rho U^2 bl} = \frac{b\int_0^l \tau_w dx}{(1/2)\rho U^2 bl} = \frac{1}{l}\int_0^l c_f dx \quad \Rightarrow C_{Df} = \frac{\sqrt{8C_1C_2}}{\sqrt{\mathrm{Re}_l}} \tag{5.10.15}$$

It may be observed from the above analysis that the functional dependence of δ and τ_w on the physical parameters is the same for any assumed velocity profile while the constants are different.

$$\frac{\delta}{x}\sqrt{\mathrm{Re}_x} = \sqrt{2C_2/C_1};\ c_f\sqrt{\mathrm{Re}_x} = \sqrt{2C_1C_2};\ C_{Df}\sqrt{\mathrm{Re}_l} = \sqrt{8C_1C_2} \tag{5.10.16}$$

Several velocity profiles may be assumed for boundary layer as shown in Fig. 5.10.2. The more closely assumed shape with the experimental data for a flat plate is the *Blasius* profile. The non-dimensional constant parameters in Eq. (5.10.16) can be evaluated through the *momentum-integral* results and given in the Table 5.10.1.

Table 5.10.1: Momentum integral estimates for a laminar flow velocity profiles

Nature of velocity profile	*Equation*	$\frac{\delta}{x}\sqrt{\mathrm{Re}_x}$	$c_f\sqrt{\mathrm{Re}_x}$	$C_{Df}\sqrt{\mathrm{Re}_l}$
Blasius	$\frac{u}{U} = f'\left(\frac{y}{\delta}\right)$	5	0.664	1.328
Linear	$\frac{u}{U} = \frac{y}{\delta}$	3.46	0.578	1.156
Parabolic	$\frac{u}{U} = \frac{2y}{\delta} - \left(\frac{y}{\delta}\right)^2$	5.48	0.73	1.46
Cubic	$\frac{u}{U} = \frac{3}{2}\left(\frac{y}{\delta}\right) - \frac{1}{2}\left(\frac{y}{\delta}\right)^3$	4.64	0.646	1.292
Sine wave	$\frac{u}{U} = \sin\left[\frac{\pi}{2}\left(\frac{y}{\delta}\right)\right]$	4.79	0.655	1.31

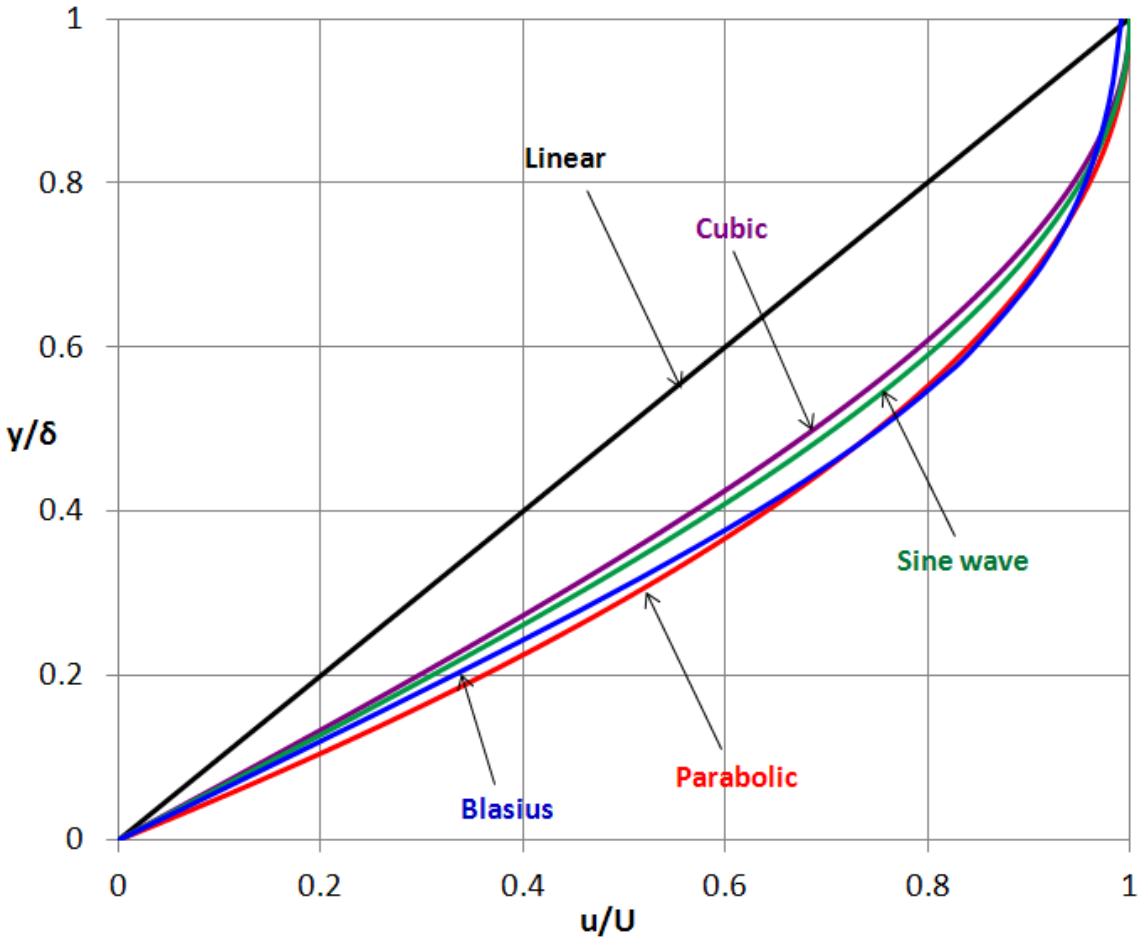

Fig. 5.10.2: Approximate boundary layer profile for momentum integral estimates.

Module 5 : Lecture 11
VISCOUS INCOMPRESSIBLE FLOW
(External Flow – Part V)

Turbulent Flat Plate Boundary Layer

A laminar boundary layer over a flat plate eventually becomes turbulent over certain range of Reynolds number. There is no unique value pf Reynolds number, for this change to happen. It mainly depends on the free stream turbulence and surface roughness parameters. With a very fine polished wall and with a quiet free stream, one can delay the transition. A controlling parameter such as the critical *Reynolds number of transition* $\left(\mathrm{Re}_{x,CR}\right)$ may be defined. On a flat plate with a sharp leading edge in a typical free stream air flow, the transition occurs between the Reynolds number ranges of 2×10^5 to 3×10^6. So the transitional Reynolds number is normally taken as $\mathrm{Re}_{x,CR}=5\times10^5$.

The complex process of transition from laminar to turbulent flow involves the instability in the flow field. The small disturbances imposed on the boundary layer flow will either grow (i.e. instability) or decay (stability) depending on the location where the disturbance is introduced. If the disturbance occurs at a location where $\mathrm{Re}_x < \mathrm{Re}_{x,CR}$, then the boundary layer will return to laminar flow at that location. Disturbances imposed on locations $\mathrm{Re}_x > \mathrm{Re}_{x,CR}$ will grow and the boundary layer flow becomes turbulent from this location. The transition to turbulence involves noticeable change in the shape of boundary layer velocity profile as shown in Fig. 5.11.1. As compared to laminar profiles, the turbulent velocity profiles are flatter and thicker at the same Reynolds number (Fig. 5.11.2). Also, they have larger velocity gradient at the wall.

There is no exact theory for turbulent flat plate flow rather many empirical models are available. To begin with the analysis of turbulent boundary layer, let us recall the momentum-integral relation which is valid for both laminar as well as turbulent flows.

$$\tau_w(x)=\rho U^2\frac{d\theta^*}{dx} \qquad (5.11.1)$$

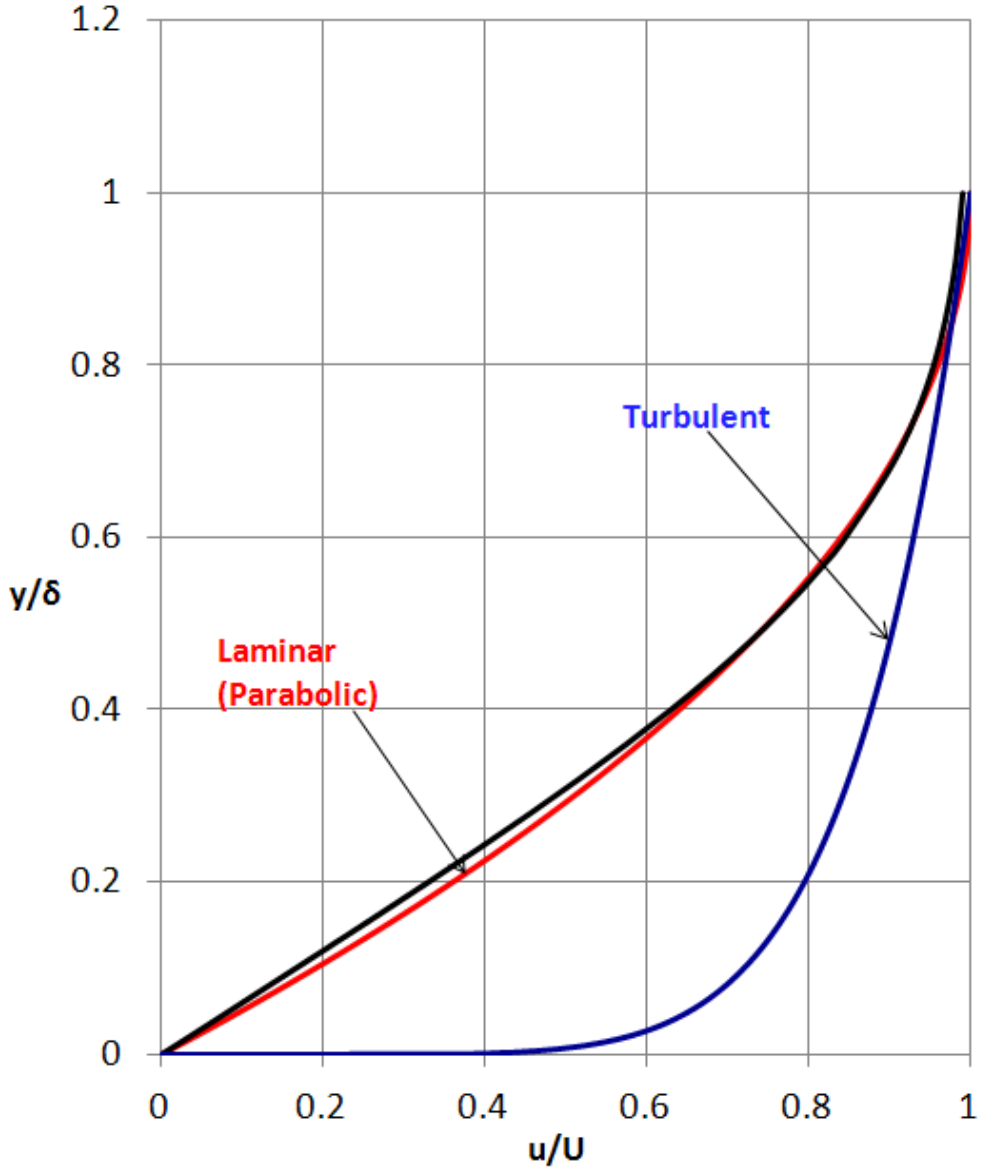

Fig. 5.11.1: Comparison of laminar and turbulent boundary layer profiles for flat plate.

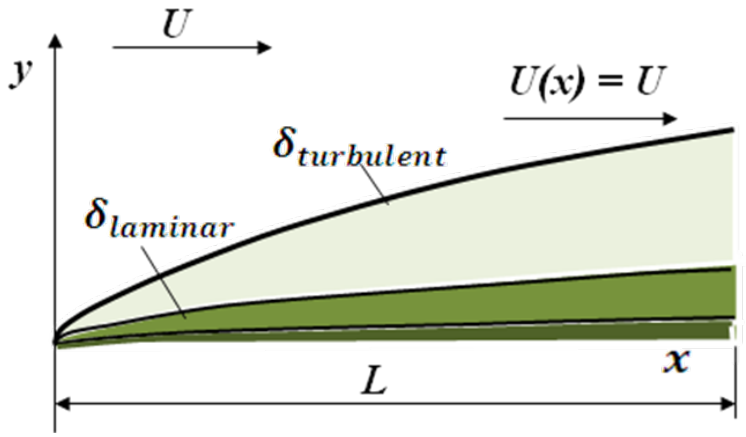

Fig. 5.11.2: Comparison of laminar and turbulent boundary layer profiles for flat plate.

In order to obtain the momentum thickness in Eq. (5.11.1), it is desired to know the velocity profile. *Prandtl* suggested the *power law* approximation for skin friction coefficient and *one-seventh power law* for velocity profile which is considered as very good approximations for flat plates.

$$c_f \approx 0.02\left(\mathrm{Re}_\delta\right)^{-(1/6)}$$
$$\frac{u}{U} \approx \left(\frac{y}{\delta}\right)^{\frac{1}{7}} \text{ for } y \le \delta \text{ and } \frac{u}{U} \approx 1 \text{ for } y > \delta \tag{5.11.2}$$

The approximate turbulent velocity profile shape given by Eq. (5.11.2) leads to the fact that the slope $\left(\partial u/\partial y\right)_{y=0}$ is infinite at the wall which is not meaningful physically. However, the large slope leads to a very high skin friction on the surface of the plate as compared to the laminar flow under similar conditions. With this approximate profile, the momentum thickness can be easily evaluated:

$$\theta^* \approx \int_0^\delta \left(\frac{y}{\delta}\right)^{1/7}\left[1-\left(\frac{y}{\delta}\right)^{1/7}\right]dy = \frac{7}{72}\delta \tag{5.11.3}$$

From the definition of skin friction coefficient and using the Eq. (5.11.1), the results are rewritten as below;

$$c_f = \frac{\tau_w(x)}{(1/2)\rho U^2} = 2\frac{d\,\theta^*}{dx} = 2\frac{d}{dx}\left(\frac{7}{72}\delta\right) \tag{5.11.4}$$

Substituting Eq. (5.11.4) in Eq. (5.11.2), separating the variables and integrating the resulting expression by assuming $\delta = 0$ at $x = 0$, the following important relation is obtained for boundary layer thickness.

$$\left(\mathrm{Re}_\delta\right) = 0.16\left(\mathrm{Re}_x\right)^{6/7} \Rightarrow \frac{\delta}{x} = \frac{0.16}{\left(\mathrm{Re}_x\right)^{1/7}} \tag{5.11.5}$$

It may be observed that the thickness of a turbulent boundary layer increases as $x^{6/7}$ while it increases as $x^{1/2}$ for a laminar boundary layer. It means that a turbulent boundary layer grows at a faster rate compared to that of a laminar boundary layer. Eq. (5.11.5) is the solution of a turbulent boundary layer because all the boundary layer parameters can be obtained from this equation as given below;

- Displacement thickness,

$$\delta^* = \int_0^{\delta}\left(1-\frac{u}{U}\right)dy = \int_0^{\delta}\left[1-\left(\frac{y}{\delta}\right)^{1/7}\right]dy = \frac{\delta}{8} = \left(\frac{1}{8}\right)\frac{0.16x}{\left(\mathrm{Re}_x\right)^{1/7}} \quad \Rightarrow \frac{\delta^*}{x} = \frac{0.02}{\left(\mathrm{Re}_x\right)^{1/7}} \tag{5.11.6}$$

- Momentum thickness,

$$\theta^* = \frac{7}{72}\delta = \frac{7}{72}\left[\frac{0.16\,x}{\left(\mathrm{Re}_x\right)^{1/7}}\right] \quad \Rightarrow \frac{\theta^*}{x} = \frac{0.016}{\left(\mathrm{Re}_x\right)^{1/7}} \tag{5.11.7}$$

- Turbulent shape factor for flat plate

$$H = \frac{\delta^*}{\theta^*} = 1.25 \tag{5.11.8}$$

- Skin friction coefficient,

$$c_f = 0.02\left(\mathrm{Re}_{\delta}\right)^{-(1/6)} = 0.02\left[0.16\left(\mathrm{Re}_x\right)^{6/7}\right]^{-(1/6)} = \frac{0.027}{\left(\mathrm{Re}_x\right)^{1/7}} \tag{5.11.9}$$

- Wall shear stress,

$$c_f = \frac{\tau_w}{(1/2)\rho U^2} = \frac{0.027}{\left(\mathrm{Re}_x\right)^{1/7}} \quad \Rightarrow \tau_w = \frac{0.0135\mu^{1/7}\rho^{6/7}U^{13/7}}{x^{1/7}} \tag{5.11.10}$$

- Drag coefficient,

$$c_d = \frac{1}{L}\int_0^L c_f\,dx = \frac{0.031}{\left(\mathrm{Re}_L\right)^{1/7}} \tag{5.11.11}$$

These are some basic results of turbulent flat plate theory. The flat plate analysis for a *Blasius* laminar boundary layer and turbulent boundary layer is summarized in Table 5.11.1.

Table 5.11.1: Comparative analysis of laminar and turbulent boundary layer flow over a flat plate

Parameters	*Laminar (Blasius solution)*	*Turbulent (Prandtl approximation)*
Boundary layer thickness	$\frac{\delta}{x}=\frac{5}{\sqrt{\mathrm{Re}_x}}$	$\frac{\delta}{x}=\frac{0.16}{(\mathrm{Re}_x)^{1/7}}$
Displacement thickness	$\frac{\delta^*}{x}=\frac{1.72}{\sqrt{\mathrm{Re}_x}}$	$\frac{\delta^*}{x}=\frac{0.02}{(\mathrm{Re}_x)^{1/7}}$
Momentum thickness	$\frac{\theta^*}{x}=\frac{0.664}{\sqrt{\mathrm{Re}_x}}$	$\frac{\theta^*}{x}=\frac{0.016}{(\mathrm{Re}_x)^{1/7}}$
Shape factor	$H=\frac{\delta^*}{\theta^*}=2.59$	$H=\frac{\delta^*}{\theta^*}=1.25$
Local skin friction coefficient	$c_f=\frac{0.664}{\sqrt{\mathrm{Re}_x}}$	$c_f=\frac{0.027}{(\mathrm{Re}_x)^{1/7}}$
Wall shear stress	$\tau_w=\frac{0.332\mu^{1/2}\rho^{1/2}U^{3/2}}{x^{1/2}}$	$\tau_w=\frac{0.0135\mu^{1/7}\rho^{6/7}U^{13/7}}{x^{1/7}}$
Drag coefficient	$c_d=\frac{1.328}{\sqrt{\mathrm{Re}_L}}$	$c_d=\frac{0.031}{(\mathrm{Re}_L)^{1/7}}$

Effect of Pressure Gradient on the Boundary Layer

The analysis of viscous flow fields past an external body (such as flat plate) is essentially done by dividing the entire flow domain in two parts; outer inviscid flow and a boundary layer flow which is predominant in the thin region close to the surface of the plate. Depending on the nature of boundary layer (laminar/turbulent), the velocity profile and all other relevant parameters are determined. However, when the outer flow accelerates/decelerates, few interesting phenomena take place within the

boundary layer. If the outer inviscid and/or irrotational flow accelerates, $U(x)$ increases and using Euler's equation, it may be shown that $p(x)$ decreases. The boundary layer in such an accelerating flow is formed very close to the wall, usually thin and is not likely to separate. Such a situation is called as *favorable pressure gradient* $\left(\frac{dp}{dx}<0\right)$. In the reverse case, when the outer flow decelerates, $U(x)$ decreases and $p(x)$ increases leading to *unfavorable/adverse pressure gradient* $\left(\frac{dp}{dx}>0\right)$. This condition is not desirable because the boundary layer is usually thicker and does not stick to the wall. So, the flow is more likely to separate from the wall due to excessive momentum loss to counteract the effects of adverse pressures. The *separation* leads to the *flow reversal* near the wall and destroys the parabolic nature of the flow field. The boundary layer equations are not valid downstream of a separation point because of the reverse flow in the separation region. Let us explain the phenomena of separation in the mathematical point of view. First recall the boundary layer equation:

$$u\frac{\partial u}{\partial x}+v\frac{\partial u}{\partial y}=U\frac{dU}{dx}+\nu\frac{\partial^2 u}{\partial y^2}=U\frac{dU}{dx}+\frac{1}{\rho}\frac{\partial \tau}{\partial y} \tag{5.11.12}$$

When the separation occurs, the flow is no longer attached to the wall i.e. $u=v=0$. Then, Eq. (5.11.12) is simplified and is valid for either laminar/turbulent flows.

$$\left(\frac{\partial \tau}{\partial y}\right)_{wall}=\mu\left(\frac{\partial^2 u}{\partial y^2}\right)_{wall}=-\rho U\frac{dU}{dx}=\frac{dp}{dx}$$
$$\text{or, } \left(\frac{\partial^2 u}{\partial y^2}\right)_{wall}=\frac{1}{\mu}\left(\frac{dp}{dx}\right) \tag{5.11.13}$$

From the nature of differential equation (Eq. 5.11.13), it is seen that the second derivative of velocity is positive at the wall in the case of adverse pressure gradient. At the same time, it must be negative at the outer layer $(y=\delta)$ to merge smoothly with the main stream flow $U(x)$. It follows that the second derivative must pass through *zero* which is known as the *point of inflection* (PI) and any boundary layer profile in an adverse gradient situation must exhibit a characteristic *S-shape*. The effect of pressure gradient on the flat plate boundary layer profile is illustrated below and is shown in Fig. 5.11.3.

Case I: Under the *favorable pressure gradient* conditions $\left(\frac{dp}{dx}<0;\ \frac{dU}{dx}>0;\frac{\partial^2 u}{\partial y^2}<0\right)$, the velocity profile across the boundary layer is rounded without any *inflection point* (Fig. 5.11.3-a). No separation occurs in this case and u approaches to $U(x)$ at the edge of the boundary layer. The wall shear stress (τ_w) is the largest compared to all other cases

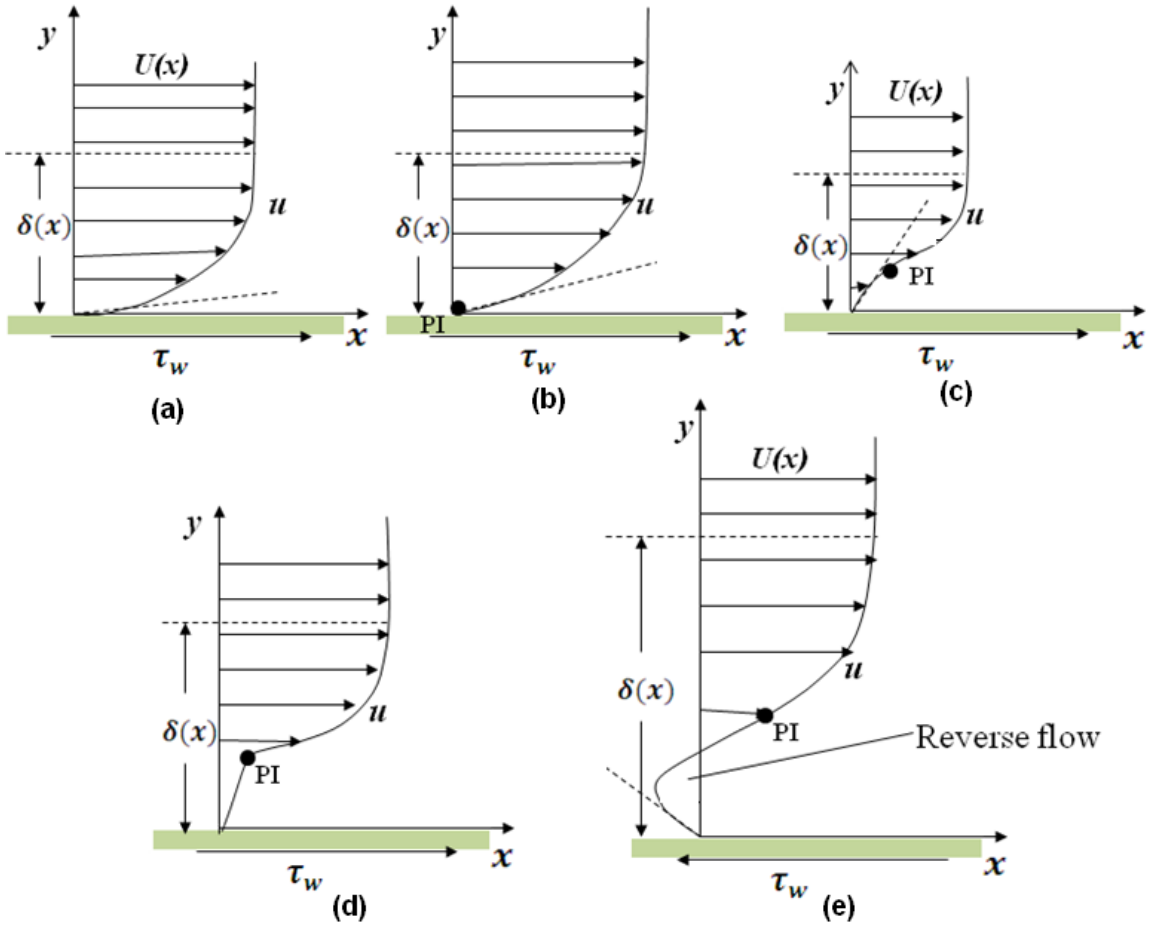

Fig. 5.11.3: Effect of pressure gradient on the boundary layer for a flat plate.

Case II: When *pressure gradient* is zero, $\left(\frac{dp}{dx}=0;\ \frac{dU}{dx}=0;\frac{\partial^2 u}{\partial y^2}=0\right)$, the *point of inflection* lies on the wall itself and there is no separation (Fig. 5.11.3-b). It implies a linear growth of u with respect to y for the boundary layer profile and is same as the *Blasius* boundary layer profile for the flat plate. The flow has a tendency to undergo the transition in the Reynolds number of about 3×10^6.

Case III: In a situation of *adverse pressure gradient* , $\left(\frac{dp}{dx}>0;\ \frac{dU}{dx}<0;\frac{\partial^2 u}{\partial y^2}>0\right)$, the outer flow is decelerated. However, the value of $\left(\partial^2 u/\partial y^2\right)$ must be negative when u approaches to $U(x)$ at the edge of the boundary layer. So, there has to be a point of inflection $\left(\frac{\partial^2 u}{\partial y^2}=0\right)$somewhere in the boundary layer and the profile looks similar to *S-shape*. In a weak adverse pressure gradient (Fig. 5.11.3-c), the flow does not actually separate but vulnerable to transition to turbulence even at lower Reynolds number of 10^5. At some moderate adverse pressure gradient, the wall shear stress is exactly zero $\left(\tau_w=\mu\left.\frac{\partial u}{\partial y}\right|_{y=0}=0\right)$. This is defined as *separation point* as shown in Fig. 5.11.3(d). Any stronger pressure gradient will cause back flow at the wall that leads to thickening the boundary layer, breaking the main flow and flow reversal at the wall (Fig. 5.11.3-e). Beyond the separation point, the wall shear stress becomes negative $(\tau_w<0)$ and the boundary layer equations break down in the region of separated flow.